Department of Chemical Engineering and Chemistry

Triplet-triplet Annihilation Upconversion in Single-Chain Polymeric Nanoparticles for Photocatalysis in Aqueous Media

Bachelor End Project

W.P.A. Verheijen   1370081

Responsible lecturer: Second assessor:
Prof. dr. ir. Anja Palmans   **Dr. Fabian Eisenreich**

Direct supervisor:
Stefan Wijker

Eindhoven, April 25, 2022

Abstract

Triplet-triplet annihilation upconversion (TTAUC) has attracted much attention due to its applications in the field of bio-imaging, photovoltaics, and photocatalysis. The upconversion is performed mostly in organic media due to the efficiency plummeting oxygen quenching process. However, for biological and green applications, the use of organic solvents should be minimized. It is shown that amphiphilic polymers can form single-chain polymeric nanoparticles (SCPNs) when dissolved in water, in which chromophores can be dissolved which creates a novel pathway for TTAUC in water. In this work, an improved sample preparation method is developed which increases the upconversion intensity. Moreover, a proof of concept is given by successfully performing a photocatalytic reaction in water utilizing the upconverted light of the chromophores dissolved in SCPNs.

Contents

1. Introduction

In triplet-triplet annihilation upconversion (TTAUC), low energetic light can be transformed into high energetic light. Applications for TTAUC include drug delivery, bio-imaging, photovoltaics, OLEDs, and photocatalysis.[1,2] It can, for instance, result in easier up-scaling of photochemical reactions, as lower frequency, non-coherent light can be used which is scattered less in materials and thus has a longer penetration depth which.[2] What is more, the low energetic light can prevent damage to living tissue which makes TTAUC also a promising technique in biomedical applications. For example, the high wavelength light could penetrate the body and can locally induce reactions within tissue.

In the field of photocatalysis, reactions are activated or accelerated by stimuli of electromagnetic radiation.[3] Here, a photocatalyst is excited by the absorption of a photon. A reaction can take place by either energy transfer or electron transfer of the excited photocatalyst to a reactant. These reactions enable to achieve new pathways to complex synthetic transformations, and surface modifications.[3] With TTAUC these processes can be scaled up, but also it could enable a pathway to a more sustainable process as even sunlight could be used for reactions. Moreover, Ravets et. al reports that with TTAUC a reaction can take place by energy transfer from the excited emitter to the reacting molecules directly without the need for a photocatalyst.[2] This reduces the number of molecules involved in one reaction which streamlines the process.

As the reduction of solvent use is seen as one of the primary goals of green chemistry, an environmentally friendly photocatalytic process ideally should be done in water.[4] The chromophores, atoms or groups of atoms that absorb light in the visible region (200-700 nm), are however often insoluble in water which complicates converting the process to aqueous media.[5,6] The use of single-chain polymeric nanoparticles (SCPNs) could mitigate these issues. An SCPN is an amphiphilic polymer in which the hydrophilic groups give solubility and the hydrophobic groups of the polymer chain cluster together when dissolved in water (hydrophobic collapse).[6] This process forms a particle with a hydrophobic pocket in the interior of the particle and a hydrophilic exterior (Figure 1.1). In this hydrophobic cavity, organic sensitizer and emitter molecules can be dissolved which can facilitate the upconversion.[7]
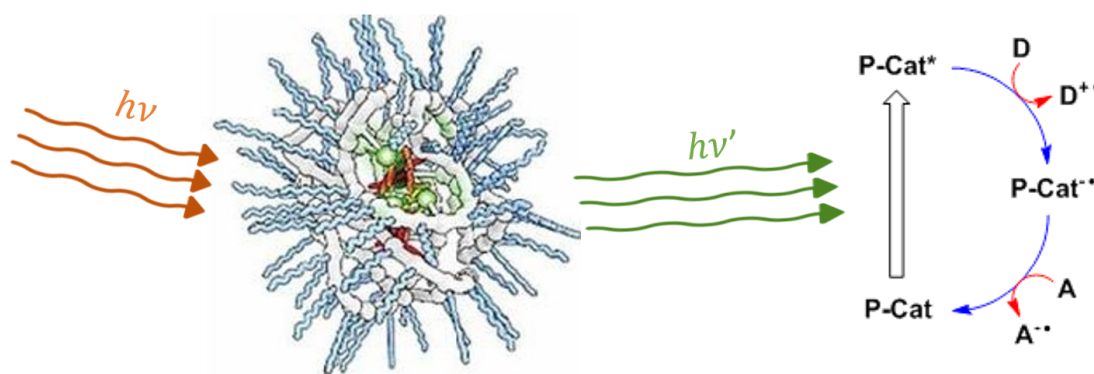

Figure 1.1.: A graphical interpretation of the TTAUC process for photo-catalysis. The red, low energy incomming light gets upconverted by the chromophores dissolved in the SCPN. Higher frequency light is emitted from the SCPN and excites a photocatalyst which can initate a photoredox reaction. Adapted from[8]

This project aims to develop a general method of dissolving the chromophores in the SCPN and optimize upconversion for photocatalysis in water. The ultimate goal is to develop a general method, in which any sensitizer and emitter pair can be selected that enables the right upconversion for the desired photocatalytic reaction. This makes the process highly tunable and thus widely applicable, and the use of water more sustainable.

This project is a continuation of the work of Van Vliet, who showed that upconversion is possible in SCPN and concluded that the SCPN can make an efficient barrier against oxygen quenching, a process that is detrimental to the efficiency of TTAUC.[7] This work investigates the possibility to utilize TTAUC in aqueous media for photocatalysis (see Figure 1.1). First, in chapter 2, the theory behind TTAUC is reviewed. Thereafter, the polymer synthesis is outlined and the results are discussed in chapter 3. In chapter 4 the optical properties and stability of chromophores are investigated and in chapter 5 the upconversion experiments are analyzed. Lastly, a photo-catalytic reaction was performed as proof of concept the results are discussed in chapter 6, followed by the conclusion 7.

2. Theory

In this chapter, the main mechanism that enables TTAUC in organic chromophores is discussed. The different steps in this process are reviewed separately to get a deeper understanding of the overall process. Thereafter, some limiting factors are given that suppress effective upconversion.

TTAUC can be schematically depicted by Figure 2.1. The process starts with the absorption of a photon by the sensitizer. Subsequently, the excited singlet state of the emitter is converted to a triplet state in intersystem crossing (ISC). Next, the energy of the sensitizer's triplet state is transferred to an emitter in a process called triplet-triplet energy transfer (TTET). When two excited emitters are in close contact, they can undergo triplet-triplet annihilation (TTA) in which the two triplet excited states are combined to obtain one high energy singlet state. When this high energy state fluoresces, a photon is emitted with a higher energy than the energy of the absorbed photons. Effectively, the energy of the two photons is thus combined.

2.1. Singlet states and triplet states

Quantum mechanics predicts that particles have discrete energy levels, with discrete angular momenta and spins.[9] Spin is quantized by the quantum numbers s and m relating to the eigenvalues of the total spin angular momentum and z component of the spin angular momentum respectively. Here m can take the values $-s, -s+1, \ldots, s-1, s$. For example a spin 1/2 particle ($s = 1/2$) can have $m = +1/2$ and $m = -1/2$ (also called spin-up $|\uparrow\rangle$ and spin-down $|\downarrow\rangle$ respectively).
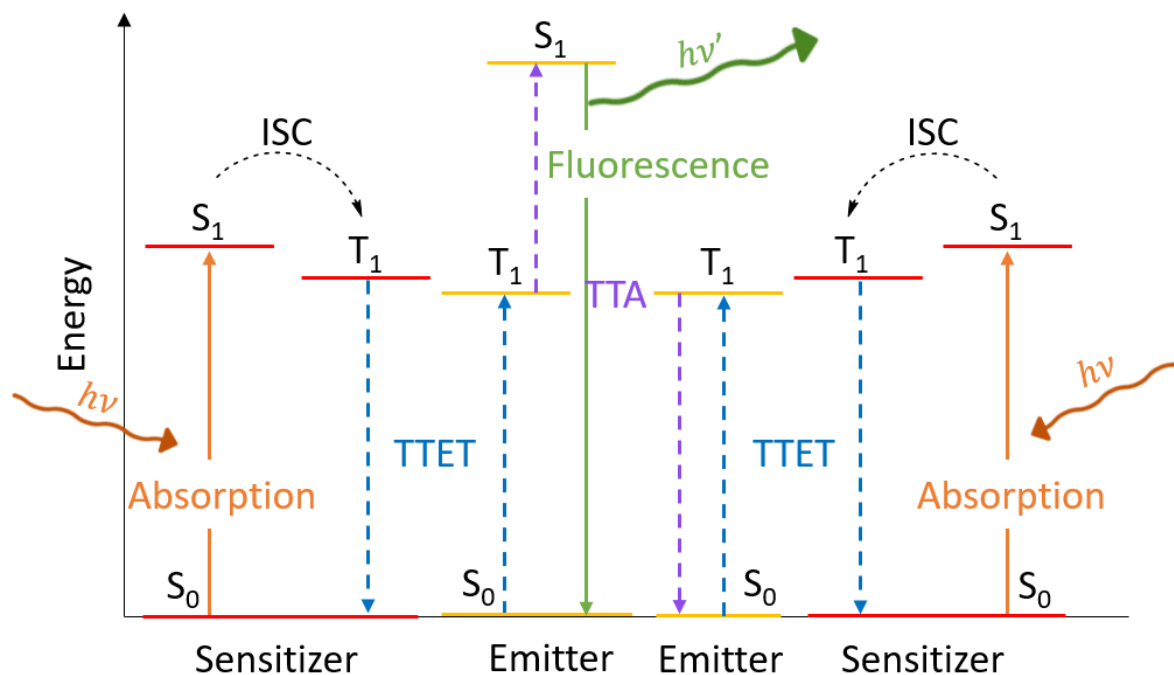

Figure 2.1.: Jablonsky diagram of TTAUC in which 2 photons are absorbed by two sensitizers, and 1 photon with a higher energy than the incomming photons is emitted by the emitter.

When two-particle systems are considered, the total angular momentum of the individual particles can be added, although, in a non-trivial manner. The total z component of the spin M, is given by the sum of the individual ones m_i:

$$M = m_1 + m_2. \tag{2.1}$$

The nett spin, however, is non-trivial and the values are

$$S = (s_1 + s_2), (s_1 + s_2 - 1), (s_1 + s_2 - 2), \ldots |s_1 - s_2|. \tag{2.2}$$

When two particles are combined (particle 1 in state $|sm\rangle = |s_1 m_1\rangle$ and particle 2 in state $|sm\rangle = |s_2 m_2\rangle$) the resulting state can be described as

$$|SM\rangle = \sum_s C^{s_1 s_2 s}_{m_1 m_2 m} |s_1\ s_2\ m_1\ m_2\rangle. \tag{2.3}$$

With $M = m_1 + m_2$, and $C^{s_1 s_2 s}_{m_1 m_2 M}$ the so-called Clebsch-Gordan coefficients (which effectively can just be looked up in tables). When for example two spin 1/2 particles are combined (two electrons for example), the possible values of S are 1 and 0. Corresponding to the states $|S\ M\rangle$

$$|1\ 1\rangle = |\uparrow\uparrow\rangle$$
$$|1\ 0\rangle = \frac{1}{\sqrt{2}} \left(|\uparrow\downarrow\rangle + |\downarrow\uparrow\rangle\right)$$
$$|1\ -1\rangle = |\downarrow\downarrow\rangle$$

for $S = 1$ and

$$|0\ 0\rangle = \frac{1}{\sqrt{2}} \left(|\uparrow\downarrow\rangle - |\downarrow\uparrow\rangle\right),$$

for $S = 0$. The $S = 1$ states have $M = 1, 0, -1$ and thus give three possible configurations, therefore, the state is called a triplet state, for $S = 0$, M can only be zero, and one configuration is possible called the singlet state. In general $2S + 1$ values of M are allowed for a state called the multiplicity.

A paired (anti-parallel) and unpaired (parallel) spin is often denoted as $\uparrow\downarrow$ and $\uparrow\uparrow$ respectively. The paired spin represents the state in which the spins cancel each other, and lead to no net angular momentum i.e. $S = 0$, the singlet state. The unpaired spin state represents the case when there is a net spin angular momentum $S \neq 0$, this leads to doublet, triplet states, etc. This may not be confused with the $m = +1/2$, and $m = -1/2$ quantum numbers, which, unfortunately, are widely denoted as up and down arrows as well. Hence all three triplet states above have an unpaired spin (S=1), which does not mean that the individual electrons have the same quantum number m (see the $|1\ 0\rangle$ state).

Hund's rules predict that the state with the highest multiplicity has the lowest energy, i.e. triplet states are lower in energy than singlet states. However, in an organic molecule, the ground state is often a singlet state. This is explained by the energy levels of the molecular orbitals in a molecule. It is most likely that a molecule has only one non-degenerate highest occupied molecular orbital (HOMO),
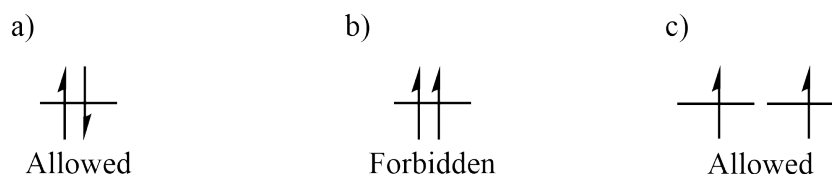

Figure 2.2.: Different configurations of the ground state in which two electrons are placed paired $\uparrow\downarrow$ or unpaired $\uparrow\uparrow$. a) The electrons are placed in the same orbital with paired spin (hence singlet state), this thus results in a total state that is antisymmetric and hence this is allowed by the Pauli principle. b) For this configuration the two electrons are occupying the same orbital with a symmetric spin state, the total wavefunction will be symmetric which is forbidden. When the ground state has two degenerate orbitals, the electrons can be both configurations c) Hund's rules predict, that the unpaired configuration of c) which maximized spin has the lowest energy.

therefore two electrons must be placed in the same orbital for the ground state. However, the Pauli principle requires that the total wavefunction of fermions must be anti-symmetric.[10] Because the two electrons are placed in the same orbital (which is thus automatically symmetric) the Pauli principle can only be satisfied if the electrons occupy an anti-symmetric spin state, which is the singlet state. Figure 2.2 a) and b)). Hence, if a molecule has a non-degenerate HOMO, the electrons must be placed in the same orbitals and the spin state must be paired resulting in a singlet state as the ground state.

When a molecule has a twofold degenerate HOMO, for example, molecular oxygen, the electrons can be placed in different orbitals, and therefore it is allowed to have an unpaired spin (see Figure 2.2 c), this results in a higher multiplicity which, leads to a lower energy according to Hund's rules and is, therefore, the ground state. So oxygen's ground state is a triplet state.

2.2. Absorption

After the discussion about singlet and triplet states of the ground state of molecules, the first process of TTAUC, absorption, will be analyzed. When photons are radiated on a molecule, an electron in the molecule can be excited in which one electron leaves the ground state and occupies an excited orbital of the molecule. This can be explained by treating the molecule as a two-level system (one ground state ψ_0, and one excited state ψ_1) and the light (polarized in the z direction) as a perturbation of the Hamiltonian of the particle given by

$$H' = -qE_0 z \cos(\omega t), \tag{2.4}$$

in which q is the charge of the electron, E_0 the strength of the electric field of the light, ω the oscillation frequency, and t the time. In this formula, the oscillation of the electric field of the light is recognized by the cosine term and the $-qE_0 z$ term as the energy of a charge q in a static electric field. From time-dependent perturbation theory, it follows that

$$H'_{10} \equiv \langle \psi_1 | H' | \psi_0 \rangle = -pE_0 \cos \omega t \tag{2.5}$$

with

$$p \equiv q \langle \psi_1 | z | \psi_0 \rangle \tag{2.6}$$

the transition dipole moment. From this a multitude of parameters can be derived. For this project the most important parameter is the probability of the transition between the ground state ψ_0 and the excited state ψ_1. This probability is proportional to the square of the transition dipole moment i.e.

$$P_{0 \to 1} \propto |p|^2. \tag{2.7}$$

The important implication is that the absorption of electromagnetic radiation by molecules only give a non-zero probability when the transition dipole moment does not vanish. Generalized in three dimensions, the initial and final state must fulfill

$$\langle \psi_1 | \vec{r} | \psi_0 \rangle \neq 0 \tag{2.8}$$

for absorption.

Because spin is an intrinsic property of a particle it is not coordinate dependent. The spin and electronic part can therefore be split and written as

$$\psi_i(\vec{r}) = \phi_i(\vec{r}) \chi_i. \tag{2.9}$$

Equation 2.8 can therefore be written as

$$\langle \phi_1 \chi_1 | \vec{r} | \phi_0 \chi_0 \rangle = \langle \phi_1 | \vec{r} | \phi_0 \rangle \langle \chi_1 | \chi_0 \rangle. \tag{2.10}$$

This result implies that if the spin state of the ground state is orthogonal to the spin state of the excited state i.e. $\langle \chi_1 | \chi_0 \rangle = 0$, the whole integral vanishes, and the probability of the transition is zero. These transitions are said to be spin-forbidden.[11,12] This is the reason why singlet to triplet transitions are not possible and why other methods should be devised to get the excited triplet states, needed for TTA.

2.3. Intersystem crossing

As discussed in the previous section, the transition between singlet and triplet states is spin forbidden and therefore cannot take place. However, when more perturbations are taken into account the transition becomes weakly allowed. The perturbation primarily responsible for intersystem crossing (ISC) is called spin-orbit coupling and can be written as

$$H' = \frac{e^2 \hbar^2}{2 m_e^2 c^2} \sum_i^n \sum_\nu^N \frac{Z_\nu^{\text{eff}}}{r_{i\nu}^3} \mathbf{S}_i \cdot \mathbf{L}_{i\nu}, \tag{2.11}$$

where e is the elementary charge, $\hbar$ the reduced Planck constant, m_e the electron's mass, c the speed of light, Z^{eff} the effective nuclear charge, a semi-empirical fit parameter, $r_{i\nu}$ the distance between nucleus ν and electron i, $\mathbf{S}$ the spin and $\mathbf{L}$ the angular momentum operator, summed over N nuclei ν, and n electrons i.[13] In equation 2.11 clearly the spin-orbit coupling can be recognised by the $\mathbf{S} \cdot \mathbf{L}$ term. Also, the fact that the perturbation is linear in the effective charge Z_ν^{eff} and proportional to $r_{i\nu}^{-3}$ gives an explanation of the fact that spin-orbit coupling dramatically increase when going from left to right in the periodic table (Z_{eff} increases r decreases). This is known as the heavy atom effect.

With Fermi's golden rule

$$k_{S \to T} = \frac{2\pi}{\hbar} \left| \langle \psi_T | H' | \psi_S \rangle \right|^2 \delta(E_S - E_T), \tag{2.12}$$

which gives the transition rate of the process from a singlet state (S) to a triplet state (T) in which E_S and E_T are the energies of the singlet and triplet state respectively, it can be derived that the transition between states with different configuration ($\langle {}^3(n, \pi^*) | H' | {}^1(\pi, \pi^*) \rangle$) have a much higher rate than transitions between states that have the same configuration ($\langle {}^3(n, \pi^*) | H' | {}^1(n, \pi^*) \rangle$ or $\langle {}^3(\pi, \pi^*) | H' | {}^1(\pi, \pi^*) \rangle$). Classically this is understood by the conservation of momentum, as the transition occurs, there is a change in spin angular momentum, to counteract this, a change in orbital angular momentum can provide a mechanism to conserve the total angular momentum of the system, therefore a change in configuration is required for the ISC.

2.4. Triplet-triplet energy transfer

When the sensitizer's singlet state S_1 is converted into a triplet state T_1 by ISC it can transfer its energy to another molecule by triplet-triplet energy transfer (TTET). There are two mechanisms of energy transfer, Förster resonance energy transfer (FRET), in which the sensitizer relaxes to the ground state while emitting a virtual photon which can be reabsorbed by the emitter via dipole-dipole couplings between the molecules.[14] This relies, however, on the absorption of a (virtual) photon by the emitter which is a $S_0 \to T_1$ transition and thus spin-forbidden. Therefore, FRET will not be the main mechanism of this energy transfer. In Figure 2.3 the mechanism of Dexter energy transfer is outlined. Here, the electrons are in such close contact that their wavefunctions overlap and a possibility arises to 'hop' from one molecule to another. The result is that the sensitizer receives a ground state electron from the emitter ending in the S_0 ground state, and the emitter receives the excited electron from the sensitizer which gives it a T_1 excited state.[15]
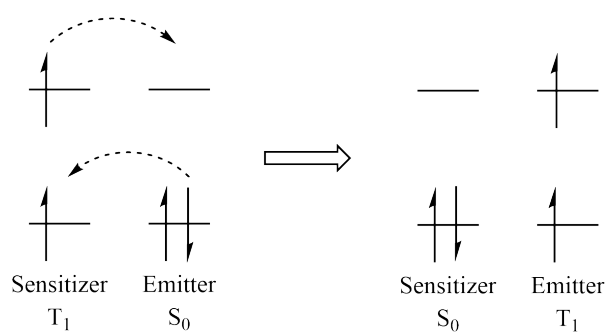
Figure 2.3.: Mechanism of TTET, in which electrons 'hop' covalently to each other. The result is that the emitter becomes excited in the T_1 state and the sensitizer relaxed in the S_0 ground state.

2.5. Triplet-triplet annihilation

The next step in the process of TTAUC is the actual triplet-triplet annihilation, in which two emitters in the triplet state are combined to produce two singlet states, one excited and one relaxed:

$$T_1 + T_1 \longrightarrow S_1 + S_0.$$
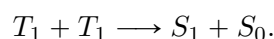
The combination of two triplet states can be seen as the combination of two particles with spin 1, forming a complex which thereafter breaks up again into separate particles. As discussed in section 2.1, the total spin of the resulting complex state can take the values $S = 2, 1, 0$. Which corresponds to a quintet state $^5(TT)^*$, a triplet state $^3(TT)^*$, and a singlet state $^1(TT)^*$ respectively. In equation form:

$$T_1 + T_1 \longrightarrow \begin{cases} ^5(TT)^* \\ ^3(TT)^* \\ ^1(TT)^* \end{cases}$$
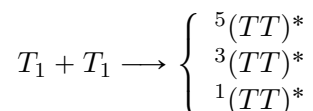
For every state $2M+1$ configurations are possible, hence there are $5+3+1 = 9$ states available, because the states are degenerate (when no magnetic field is applied, and ignoring spin-orbit interactions), all states have equal probability. When the complex breaks up back into two individual particles, the exact reverse process will take place. To conserve the spin S in this process, this leads to the following states[16]

$$^5(TT)^* \longrightarrow Q_1 + S_0$$
$$^3(TT)^* \longrightarrow T_1 + S_0$$
$$^1(TT)^* \longrightarrow S_1 + S_0$$
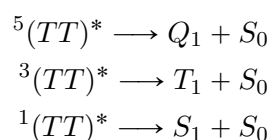
As all nine states are degenerate, the probability of a quintet ($S = 2$), triplet ($S = 1$), and singlet ($S = 0$) are given by 5/9, 3/9, and 1/9 respectively.[17] Therefore, the required singlet end-state only will form in 11% of the decays. This, however, is much lower than experimentally observed. An explanation for this is that the quintet state is too high in energy and is therefore inaccessible for TTA and the quintet state will transform back into two triplet states.[18,7] Ignoring the quintet state increases the probability of the TTA to 2/5. However, more advanced models could predict come closer to experimental data.[17]

Because TTA involves two emitters, the rate of the process is quadratically proportional to the concentration of excited emitters, which is proportional to the number of photons absorbed (absorption, ISC, and TTET are all dependent on 1 particle species only). Hence the upconversion should depend quadratically on the incoming light intensity.

2.6. Quantum yield

Apart from the discussion about the working principles of TTAUC, also the efficiency of these processes should be taken into account. The total quantum yield of TTAUC, defined as the ratio of the number of upconverted excited states and photons absorbed by the sensitizer.[19] Which can be written as

$$\Phi_{UC} = \frac{1}{2}\Phi_{ISC}\Phi_{TTET}\Phi_{TTA}\Phi_{fl}, \tag{2.13}$$

Where f is the statistical probability of formation of a singlet state in TTA, Φ_{ISC}, Φ_{TTET}, Φ_{TTA} and Φ_{fl} the quantum yield of intersystem crossing, TTET, TTA, and fluorescence of the upconverted emitter respectively.[20] Another important parameter in TTAUC is the power density threshold I_th, defined as the photon flux at which 50% of Φ_{UC} is achieved. Lastly, the Stokes shift, the energy difference between incoming and upconverted photons, should ideally be maximized.

At first sight, TTET would be maximized by minimizing the energy gap between triplet states of sensitizer and emitter. This would maximize the resonance between the molecules and with it dexter energy transfer resulting in high TTET rates and low thermalization losses.[21] Nevertheless another process, apart from regular TTET from the sensitizer's T_1 state to the emitter's T_1 state, the reverse process will be boosted as well. This reverse triplet-triplet energy transfer (R-TTET) competes with the regular TTET and limits the number of triplet states of the emitter that can undergo TTA, and is thus seen as a detrimental process.

Therefore, two conditions are discussed to limit R-TTET. First of all, from the equilibrium condition

$$K_{eq} = \frac{k_{TTET}}{k_{R-TTET}} = \exp\left(-\frac{\Delta E}{k_B T}\right), \tag{2.14}$$

in which K_{eq} is the equilibrium constant, k_{TTET} and k_{R-TTET} are the rate constants of the forward and reverse TTET respectively, ΔE the energy difference between the sensitizer's and emitter's T_1 energy levels, k_B the Boltzmann constant, and T the temperature, it can be seen that the forward process must be exothermic, meaning that the energy level of the emitter's T_1 state must be lower in energy than the emitter's triplet state, to drive the equilibrium towards the forward TTET.[22] Secondly, the entropy gain of the process, given by

$$\Delta S = k_B \ln\left(\frac{[E_0][S_T]}{[S_0][E_T]}\right), \tag{2.15}$$

where $[E_0]$, $[E_T]$, $[S_0]$, and $[S_T]$ are the concentration of the ground state emitter, triplet state emitter, ground state sensitizer, and triplet state sensitizer respectively, could be maximized by maximizing the concentration of ground state emitters.[23] In other words, the probability of an excited emitter to collide with a sensitizer molecule and undergo R-TTET is minimized. Therefore high ratio's of emitter to sensitizers are used for TTAUC.

Another important process limiting Φ_{UC} is oxygen quenching. Here, an excited triplet state can be quenched by molecular oxygen as it has a triplet ground state itself. Oxygen has a ground state configuration of (core electrons)$(\pi_x)^2(\pi_y)^2(\pi_x^*)^1(\pi_y^*)^1$. Because the π_x^* and π_y^* HOMOs are degenerate, the triplet state (as given in Figure 2.2 c) is the lowest in energy by Hund's rules. Hence, molecular oxygen has a triplet ground state (T_0). When a T_0 oxygen collides with an excited state triplet state T_1, TTET can also occur here and the oxygen is excited to a singlet state S_1 which simultaneously quenches the excited triplet state in the S_0 ground state.[5] The generated singlet oxygen is a highly reactive species, which can oxidize the chromophores reducing the efficiency of the process even further.[1]. As this process is disastrous for Φ_{UC}, minimizing oxygen quenching is of high research interest. Oxygen quenching can be reduced by degassing the solution, but more techniques can be applied to this

end. Micelles, polymers, oxygen scavengers, and Lanthanide containing upconversion nanoparticles all can result in less quenching. [24,1,25]

The formation of excimers or exciplexes, complexes of one excited and one ground state species that combine their orbitals to stabilize the excited state, can result in a loss in TTAUC as well. Here, excimers and exciplexes are complexes with two of the same or two different molecules respectively. The stabilized excimer has a lower overall energy and will thus not undergo TTET readily, which limits the overall Φ_{UC}. As the formation of exciplexes is controlled by the concentration of the components, the formation of these exciplexes can be reduced by decreasing the concentration of the components in solution. The presence of the complexes can be recognized by extra peaks in the absorbance and emission spectra that do not comply with the spectra of either of the individual components in the solution, and by a concentration dependence of these peaks. [5]

The last factor that will be discussed that reduces the quantum yield is re-absorption. When the emitter emits in the same wavelength as the sensitizer absorbs, reabsorption is observed which limits the number of upconverted photons that can be utilized.

With all this in mind, it is clear that, emitter and sensitizer should have a very specific energy level alignment, such that, the triplet states lie close in energy, but the triplet state of the emitter should lay lower than the sensitizer for efficient TTET. Moreover, the sensitizer should have a fast ISC rate and a long triplet state lifetime. The S_1 state of the emitter should be higher in energy than the S_1 state of the sensitizer will there be any anti-stokes shift of the emitted photons. Lastly, the absorption spectra of the emitter should not overlap with the fluorescence spectrum of the emitter.

3. Polymer synthesis

In this project, several varieties of the polymer depicted in Figure 3.1 are used. The polymers have different fractions of the hydrophilic Jeffamine (**JEF**), and hydrophobic dodecyl (**DD**) groups attached to the backbone of the polymer. Also, two different degrees of polymerization (DP) were used. The different varieties of polymer are given in Table 3.1. It is thought that the amount of hydrophobic side-chains in the polymer changes the behavior of the formed SCPN in water. When no hydrophobic dodecyl grafts are built-in, the polymer is well dissolved in water, however no hydrophobic collapse will take place. With the addition of dodecyl groups, the polymer will undergo the hydrophobic collapse in water, however, due to the lower solubility, the chance of aggregation will increase as well. Similarly, when the DP of the polymer has increased, the size of the hydrophobic pocket will increase. Therefore, a balance between the dodecyl and Jeffamine should be found, however, as too many hydrophobic groups could lead to aggregation. In this project **P1-P3** are synthesized using the route of Figure 3.2. **P4-P6** were synthesized in parallel by Stefan Wijker and ready to use. **P7** was a year-old polymer synthesized by Fabian Eisenreich used for initial experiments. Firstly, the mechanisms behind the synthesis are reviewed. The experimental proceedings are discussed subsequently, whereafter the characterization of the polymers will be covered.
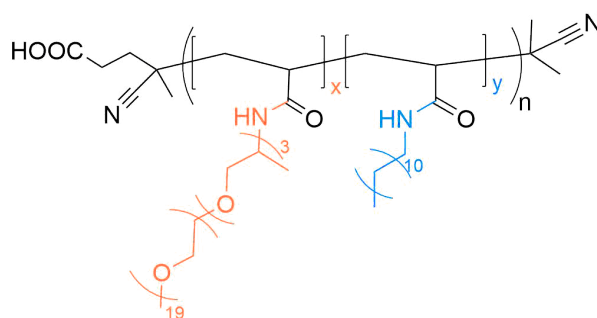

Figure 3.1.: Polymer used for SCPNs in the project, orange grafts originate from Jeffamine, blue from dodecyl. The fraction of dodecyl x and Jeffamine y was changed as well as the degree of polymerisation n to obtain different varieties of polymers.

Table 3.1.: Polymer varieties that were aimed for in the project, ∗**P7** is an old polymer that was available in a large quantity on which the initial experiments were done.

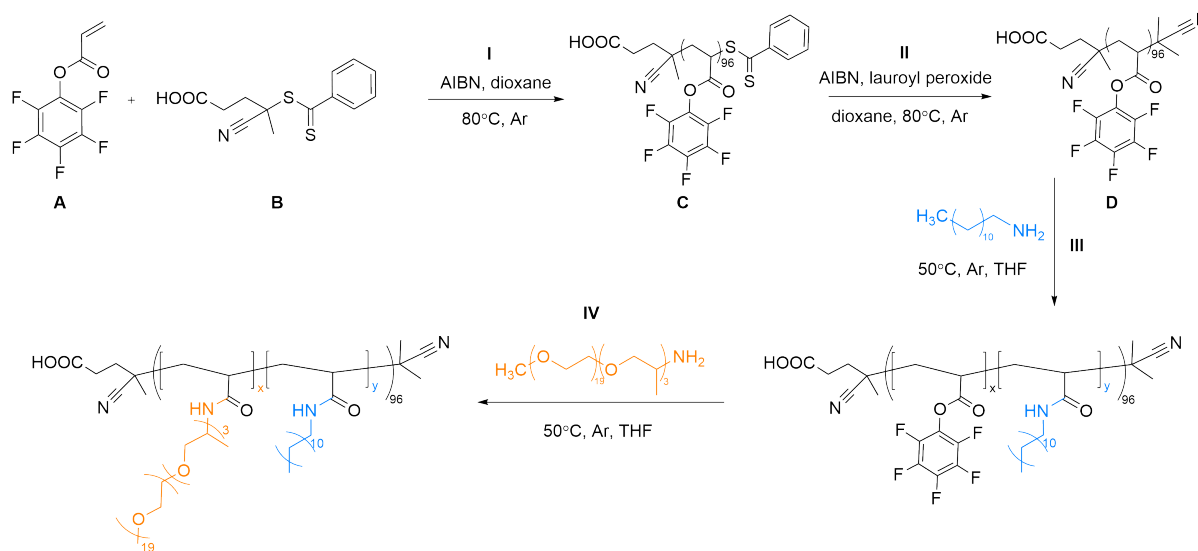| Polymer	n	x (%)	y (%)
P1	100	20	80
P2	100	30	70
P3	100	40	60
P4	200	20	80
P5	200	30	60
P6	200	40	40
P7∗	100	20	80

Figure 3.2.: Polymer synthesis of **P1-P3**

3.1. Theory

3.1.1. RAFT - polymerization

A reversible additionfragmentation chain-transfer (RAFT) polymerization is used to synthesize the backbone of the polymer (reaction **I** in Figure 3.2). A RAFT polymerization is a living polymerization which means that chain growth is not terminated and no irreversible chain transfer is present.[7,26,27] Also, the active centres of the growing macromolecule can be temporarily deactivated. The polymer chains alternate in growing. In this way, a polymer with a small molecular weight distribution, or dispersity Đ, can be obtained.

The polymerization starts with the creation of radicals. This is achieved by thermal decomposition of azobisisobutyronitrile (AIBN) as depicted in Figure 3.3.[28] The formed radicals react with the monomer, pentafluorophenyl acrylate, following Figure 3.4 in the initiation step to create an active center which can act as a start for chain-growth.
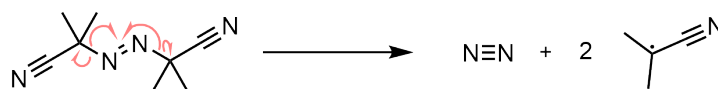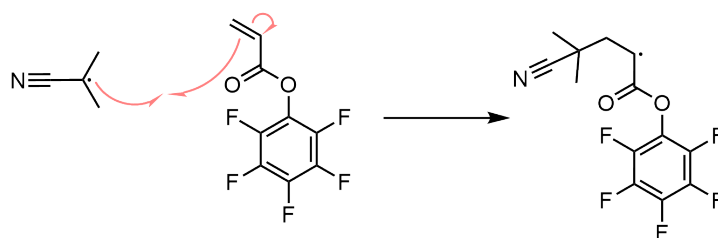

Figure 3.3.: Dissociation of AIBN

Figure 3.4.: Initiation

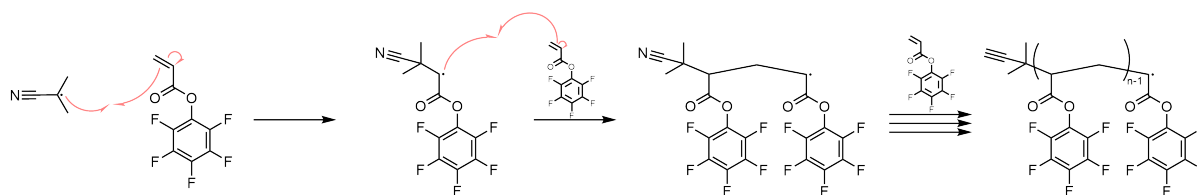The radical site on the monomer can undergo a propagation reaction as depicted in Figure 3.5.

Figure 3.5.: Propagation

Simultaneously, an equilibrium reaction with the growing polymer chain and the, so-called RAFT agent (**B**) is reached as given in Figure 3.6. In this equilibrium, the chain growth is temporarily halted. This is called the pre-equilibrium of a RAFT polymerization.
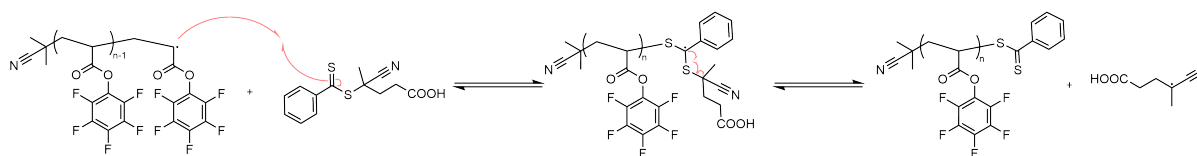
Figure 3.6.: Pre-equilibrium

The new radical formed can, again, initiate a new polymerisation as depicted in Figure 3.7. Subsequently, this chain can undergo propagation again (see Figure 3.8).
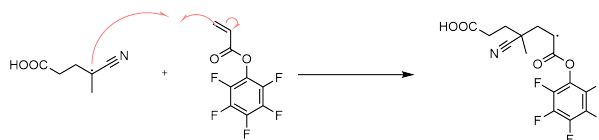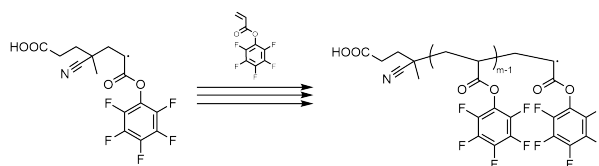
Figure 3.7.: Re-initiation

Figure 3.8.: Propagation

The reversible chain transfer part of the RAFT polymerization is explained by the reaction equilibria of Figure 3.9. Here, one growing chain (with a radical site) is attached to the RAFT group, which temporarily stops the chain growth for this polymer branch. Moreover, the chain that was attached to the RAFT agent can be eliminated as seen in the second equilibrium. Thereafter, this chain will polymerize further as depicted in Figure 3.8. The reactions of Figure 3.9 are very fast. This ensures that every chain can grow at the same rate, and thus a similar size to every polymer chain.
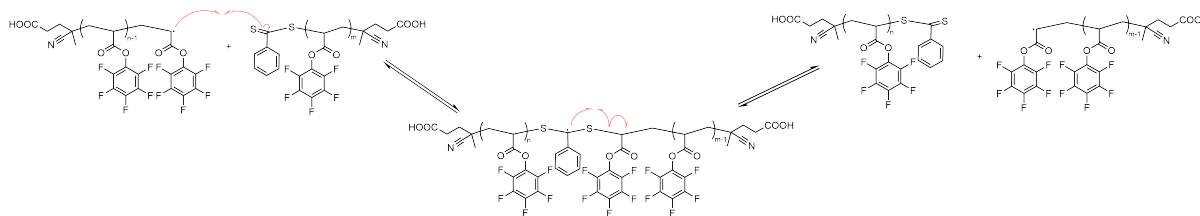
Figure 3.9.: Main-equilibrium

The last step in the RAFT polymerization is the termination of the reaction. Two growing polymer chains can be terminated by the reactions of Figure 3.10. However, because this reaction is a living polymerization, the termination step is occurring only in very small amounts, and the termination products are not the main product. Typically, the reaction will be stopped at around 70% conversion. This ensures a low dispersity as very little chain-chain coupling has occurred and every polymer chain had equal chances to grow due to the RAFT equilibria.

The polymerization is stopped by quenching in liquid nitrogen. This lowers the internal energy of the system and by solidification of the solution, the mobility of the molecules is dramatically decreased. This would stop the reactions from occurring, moreover, oxygen is allowed to flow in, which inhibits the propagation of the polymer as well. The oxygen reacts with the carbon radicals forming peroxy radicals and hydroperoxides, which are not efficient at reinitiating the polymerisation.[29]
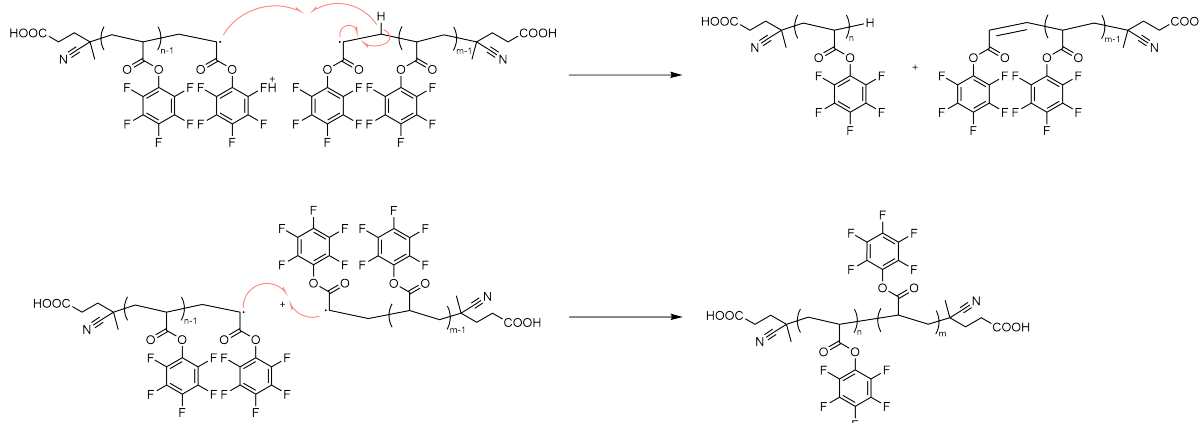

Figure 3.10.: Termination

3.1.2. Deprotection of RAFT-group

After the polymerization, the RAFT-group, attached to the backbone of the polymer, is still reactive, therefore deprotection is required. This is achieved by letting the polymer react with an excess (20 times the polymer concentration) of initiator (AIBN), in the presence of lauroyl peroxide as given in Figure 3.11.[30] In this reaction, the O–O-bond of the lauroyl peroxide will be dissociated into two equal parts. This intermediate is unstable and will eliminate CO_2. This results in a highly reactive primary radical that can attack the RAFT group on the polymer. The polymer chain is subsequently eliminated from the RAFT group, however, the equilibrium is shifted towards the product side because the undecyl is a very bad leaving group. Meanwhile, the excess AIBN is dissociated as given in Figure 3.3, which reacts with the polymer radical in a termination step to give the deprotected polymer. The product is stable and will not reform into a radical. Using lauroyl peroxide decreases the chain-chain coupling reaction with two radical polymer chains (the bottom reaction in Figure 3.10) and drives the reaction to completion due to the creation of the very reactive undecyl radical.
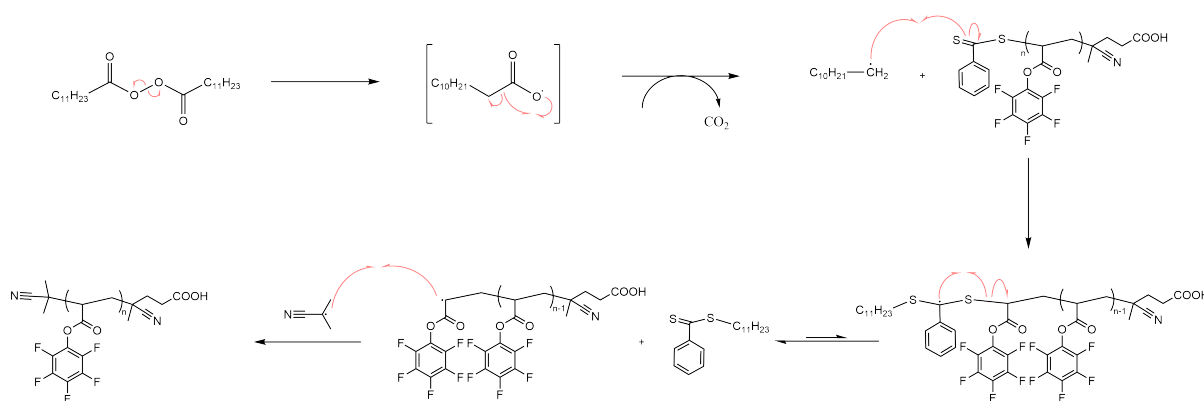
Figure 3.11.: Deprotection of RAFT group.

3.1.3. Side group modification

Now that the backbone of the polymer is synthesized the pentafluorophenoxy groups can be substituted by an aminolysis reaction. Because the fluorine inductively withdraws electrons, and by resonance in the ring, the negative charge is stabilized and hence the pentafluorophenoxy group is a good leaving group. The amine acts as a nucleophile and can attack the carbonyl carbon, creating the well-known tetrahedral intermediate, subsequent elimination of the good leaving group, and lastly, deprotonation of the nitrogen leaves an amide bond. [31]

Firstly an accurately known amount of dodecylamine reacts with the polymer to build in the dodecyl grafts via an aminolysis mechanism (Figure 3.12). Thereafter an excess of Jeffamine M1000 is reacted with the polymer to substitute the remainder of the pentafluorophenoxy groups (see Figure 3.13). In this reaction, the previously built-in dodecyl groups will not react as the amine is a stronger base than the pentafluorophenol and therefore a poor leaving group in the reactions with carbonyl compounds.
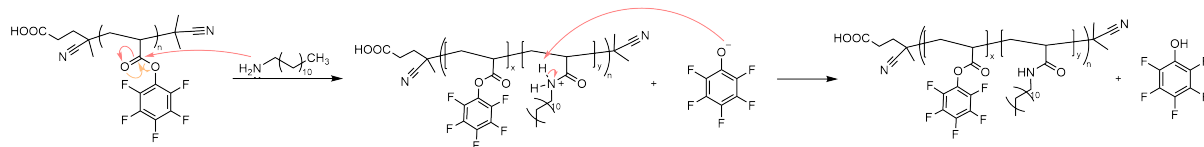

Figure 3.12.: Aminolysis mechanism to modify the polymer backbone with dodecyl units.
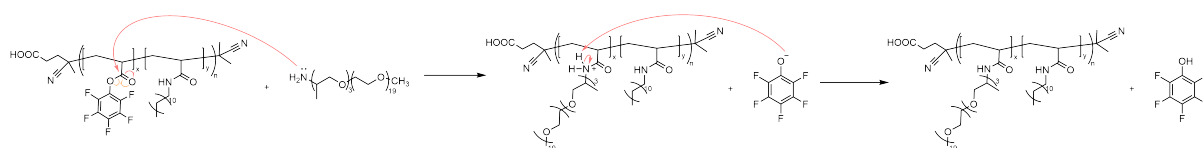

Figure 3.13.: Aminolysis reaction to finish the polymer synthesis substituting the remaining pentafluorophenoxy groups with Jeffamine units.

This concludes the discussion about the mechanisms of the performed reaction, in the next section the experimental details are given followed by the characterization of the synthesized polymers.

3.2. Results

The first step in the synthesis, as described in section 3.1.1, is the RAFT-polymerisation of the pentafluorophenyl acrylate (PFPA, **A** Figure 3.2). The conversion was checked with ^{19}F NMR at 1 h and 10 min and 1 h and 40 min, and 1 h and 45 min. The results are given in Figure 3.14. The conversion of the reaction could be determined from the integrals between the b and e peaks and c and f peaks in the figure. After 1 h and 10 min the conversion was 53%, after 1 h and 40 min 63%, and the final conversion, after 1 h and 45 min was calculated to be 67%. Therefore the degree of polymerization could be calculated by

$$DP = X \cdot \frac{n_{\text{PFPA}}}{n_{\text{RAFT}}}, \tag{3.1}$$

with X the conversion of the reaction, n_{PFPA} and n_{RAFT} the number of moles of PFPA and RAFT-agent (**B**) used in the reaction respectively. This resulted in DP = 96, hence the reaction was stopped slightly too early, as the aim was a DP = 100 polymer. The amount of PFPA after precipitation was monitored with ^{19}F NMR as well. After the second precipitation no traces of monomer could be found (see Figure A.1). Size exclusion chromatography (SEC) in THF gave a dispersity of Đ = 1.2 (see Figure A.2). Fourier transform infra-red (FTIR) spectroscopy on the solid sample showed sharp peaks at $\tilde{\nu} = 1783$ cm^{-1} and 1516 cm which could be attributed to the phenyl ester, and pentafluorphenyl group respectively (see Figure A.3) .[32] Lastly, ^{1}H NMR showed three broad polymer peaks (see Figure A.4) at $\delta = 3.08$, 2.49 $2.62 - 1.85$ ppm of which the first could be allocated to the single proton on the polymer chain and the latter two, to the two protons on the other carbon of the polymer chain.

The next synthesis step was the deprotection of the RAFT group. In this reaction, a color change was observed from pink to colorless which was an indication that the RAFT group successfully was cleaved from the polymer. After every precipitation the amount of AIBN left in the polymer solution
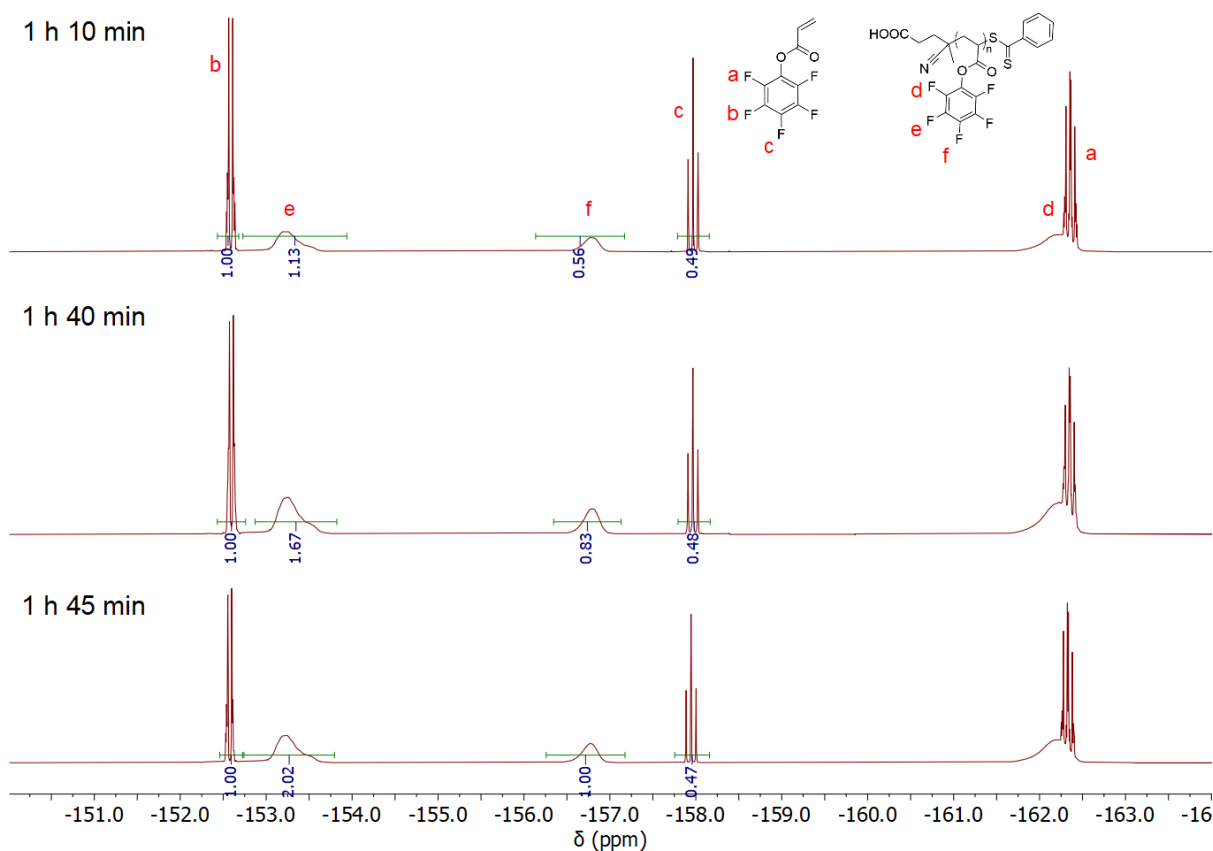

Figure 3.14.: ^{19}F NMR spectra of **C** to monitor the conversion of the RAFT-polymerisation.
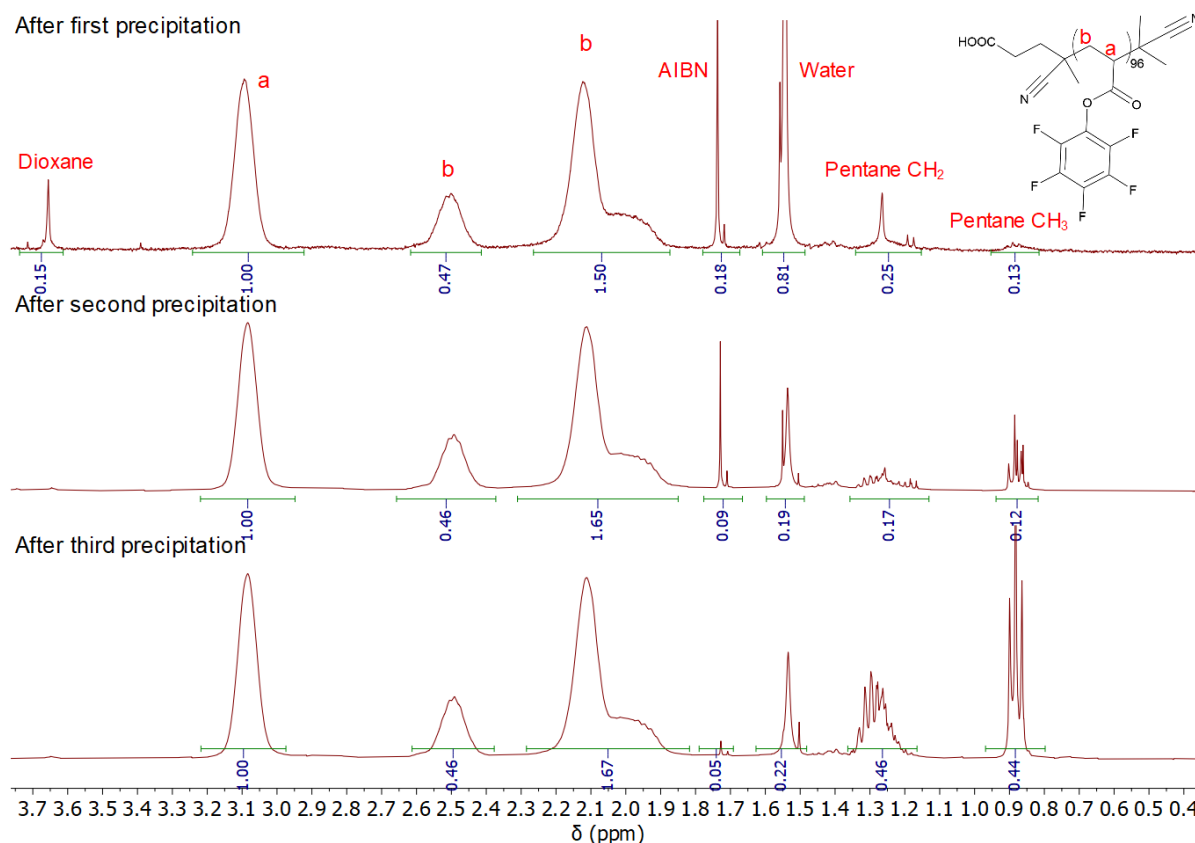
Figure 3.15.: ^{1}H NMR spectra taken after every precipitation step for **D**.

was monitored with ^{1}H NMR ($\delta = 1.73$ ppm), the results are depicted in Figure 3.15. Here the AIBN peak decreases every precipitation step, after the second precipitation the amount of AIBN was found to be 9% of the peak. As the amount of AIBN aimed for was 5% or less, another precipitation step was performed. After which it was concluded that enough AIBN was separated from the polymer. After drying the polymer, the final product was characterised with ^{1}H NMR (Figure A.5) and from SEC in THF (Figure A.6) the dispersity of **D** was determined to be $Đ = 1.2$, similar to **C**.

The side-group modification of the polymer with dodecyl, reaction III of Figure 3.2, was performed overnight. From the ^{19}F NMR spectra that were taken after 21 h of reaction (3.16), the amount of dodecyl in the polymer could be determined from the ratio of pentafluorophenyl acrylate and pentafluorophenol peaks in the ^{19}F NMR spectra. This resulted in a dodecyl content of 22%, 33%, and 44% for **P1**, **P2**, and **P3** respectively (see Table A.1). The feed ratio was 20%, 30%, and 40% respectively, so somewhat more dodecyl was built-in than expected. The ratio between the c and f peaks of the spectra were considered too small for **P1** to give an accurate result, therefore these were not taken into account with averaging. Also, the manual correction and baseline correction applied to create these spectra show to have a considerable ($\pm 2\%$) influence on the results, so there is an uncertainty in these results.

The last step of the synthesis was performed, subsequently, which was adding the Jeffamine to react. To check if all Jeffamine had reacted an ^{19}F NMR spectrum was taken on the reaction mixtures (Figure A.7) in which no broad peaks of the pentafluorophenyl acrylate in the polymer could be recognized, and only peaks coming from the pentafluorophenol. The pentafluorophenol and unreacted monomer were removed by dialysis. The absence of pentafluorophenol peaks in ^{19}F NMR confirmed its successful removal. The final yield of the end product was 278 mg, 240 mg, and 299.6 mg. Products **P1-P7** were characterized using ^{1}H NMR (Figure A.8-A.14), IR (Figure A.15, not measured for **P7**), SEC in dimethylformamide (DMF) (Figure A.16, not measured for **P7**) and phosphate-buffered saline (PBS,
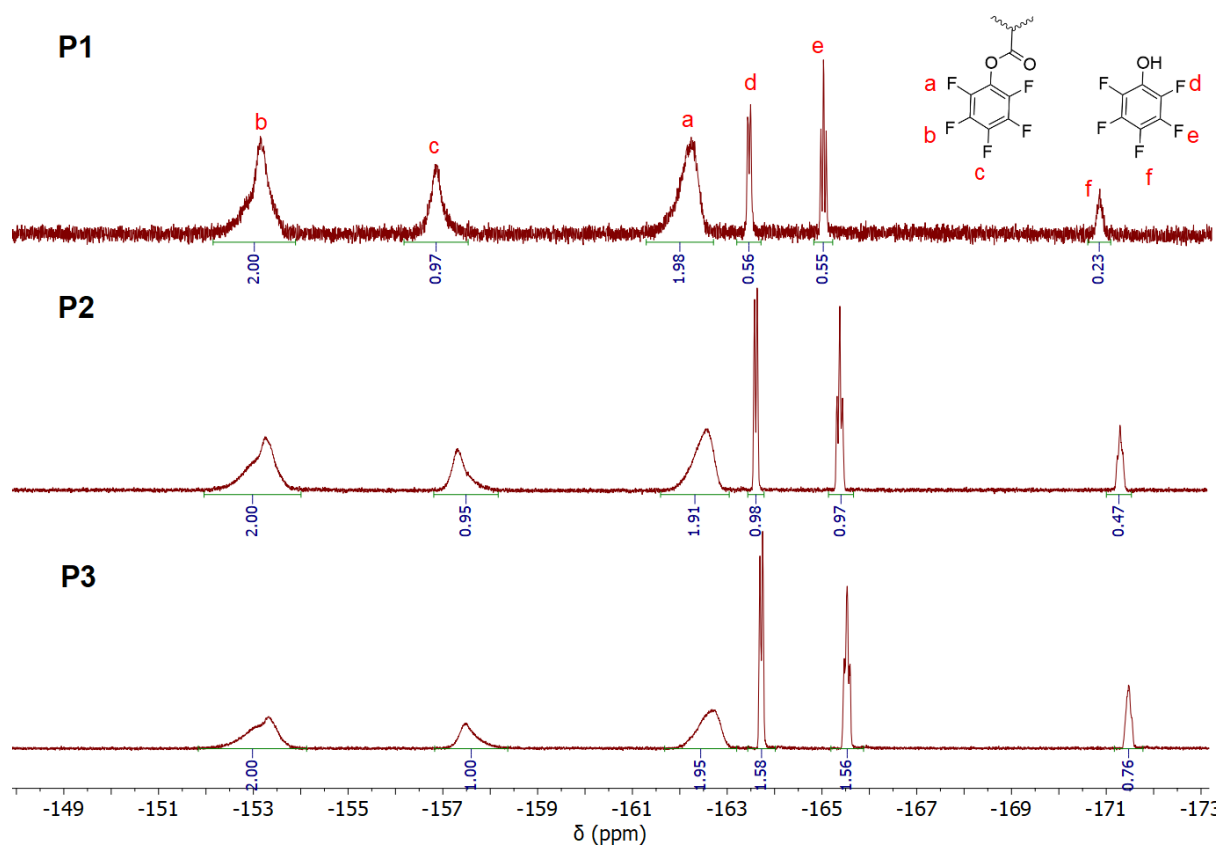
Figure 3.16.: ^{19}F NMR after reaction of **D** with dodecyle amine. From these spectra, the fraction of doeceyle moyeties in the polymer could be determined.

Figure A.17), and dynamic light scattering (DLS) to characterize the SCPN formation.

The SEC results are summarized in Table 3.2, where it can be seen that the **P3** and **P6**, the polymers with the most Jeffamine content, have a higher dispersity than the other polymers. This difference is larger in PBS than in measurements done in DMF.

Table 3.2.: Summary of results from SEC measurements in DMF and PBS.

Polymer	Đ (-) DMF	Đ (-) PBS
P1	1.2	1.4
P2	1.2	1.4
P3	1.3	1.6
P4	1.4	1.4
P5	1.4	1.4
P6	1.4	1.7
P7	-	1.5

In Figure 3.17, the size distribution is given for the polymer in water. The polymers form particles around 10 nm in diameter which is an indication that the polymers undergo the hydrophobic collapse and form SCPN.[33,34,35] The hydrodynamic diameters that were extracted from the DLS measurements are given in Table A.2. From both Figure 3.17 and the hydrodynamic diameter of the largest intensity peak out of Table A.2, it is noticed that **P7** does not form well-defined nano-particles, and aggregates are present in the solution. Also from the ^{1}H NMR (Figure A.14 extra peaks are recognized in comparison with **P1** which should have the same structure and thus spectra as **P7**. These extra peaks

before the Jeffamine protons could be an indication that the polymer is degrading. The fact that no stable solution could be maintained for more than a day and that aggregates are formed in this time, makes that the polymer is not pure anymore and should not be used for experiments where clear well-dissolved polymer solutions are necessary. This conclusion, however, was drawn after many of the experiments described in chapter 5 were done. Therefore, care must be taken in the interpretation of these results.
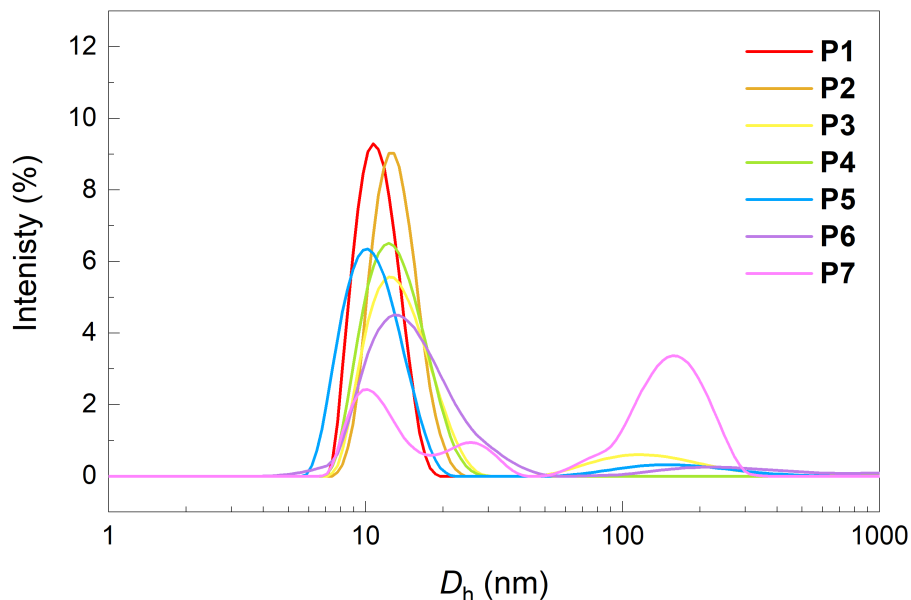

Figure 3.17.: DLS measurements on **P1**-**P7** in water ($c = 1$ mg/mL, filtered with a 0.2 μm PVDF filter)

In conclusion, three amphiphilic polymers (**P1-P3**) were successfully synthesized and characterized. The target characteristics of the polymer (as given in Table 3.1) were achieved reasonably well and the actual parameters are summarized in Table 3.3.

Table 3.3.: Polymer varieties used in the project, * assumed values.

Polymer	n	x (%)	y (%)
P1	96	22	78
P2	96	33	67
P3	96	44	56
P4	197	22	78
P5	197	34	66
P6	197	46	54
P7*	100	20	80

3.3. Experimental

3.3.1. General procedures

All commercial compounds and solvents were used as received without further purification. Solvents are bought from Biosolve unless stated otherwise. Methanol-d_4, and deuterium oxide were purchased from Sigma-Aldrich, other deuterated solvents were purchased from Cambridge Isotope Laboratories, Inc. Dry solvents were collected from an MBraun solvent purification system (MB-SPS-800). All water used in the experiments was taken from a Milli-Q ultrapure water purification system.

NMR spectra were taken using a Bruker 400 MHz Ultrashield spectrometer at ambient temperature. Chemical shifts (δ) are reported in parts per million (ppm) and were given by residual protonated solvent signals as internal standard for ^{1}H NMR (Residual proton peaks ^{1}H: δ(CDCl$_3$) = 7.26 ppm, δ(D$_2$O) = 4.79 ppm, δ(CD$_3$OD)=3.30 ppm). The residual solvent signals are. Multiplicity is reported as: s = singlet, d = doublet, t = triplet, q = quartet, m = multiplet, and br = broad. ^{19}F NMR was taken with a recycle delay of 10 s for more accurate integration. Size exclusion chromatography (SEC) was done for THF and DMF (stab. 10 mM LiBr) as eluent on a Shimadzu LC-2030C liquid chromatography system and for PBS as eluent on a Shimadzu LC-2050C liquid chromatography system. Samples were always filtered beforehand with a Whatman 0.45μm PTFE, 0.45μm regenerated cellulose, or 0.2 μm PVDF filter for THF, DMF, and PBS respectively. FTIR was done on a PerkinElmer FT-IR Spectrum Two in ATR mode. Dynamic light scattering (DLS) experiments were performed on a Malvern V Zetasizer equipped with an 830 nm laser and a 90° scattering angle. Samples were measured in Sarstedt UV-transparent disposable cuvettes with a path length of 10x2 mm. Measurement data were analyzed with Zetasizer software. UV-vis absorbance spectra were obtained from an Aligent Cary 3500 UV-vis Multicell Peltier spectrometer (averaging time 0.020 s, data interval: 1.00 nm, scan rate: 3000 nm/min, spectral bandwidth: 1.00 nm, measurement range: 200-900 nm). Fluorescence and up-conversion measurements were performed on an Aligent Cary Eclipse fluorescence spectrophotometer (Excitation slit: 5nm, emission slit: 5 nm, scan speed: 600 nm/min, excitation filter: auto, emission filter: open, intensity: 800 V unless stated otherwise, for fluorescence spectra of emitters the intensity was changed to 600V), or, when specified, an FLSP 920 double-monochromator fluorescence spectrometer from Edinburgh Instruments. QS High precision cells quartz cuvettes were used with a septum screw cap when the solution was degassed (path length 10×10 mm).

Drying of glassware was done in a 140°C oven overnight. Dialysis of polymer samples was carried out in Spectra/Por® Standard RC Tubing with a molecular weight cutoff of 6-8 kDa. All chromophore and polymer solutions were stored in the dark, and under argon. Degassing was done by bubbling the solution vigorously with argon for the given amount of time.

Jeffamine® M-1000 was kindly provided by Huntsman B.V., platinum octaethylporpherin from Porhy-Chem, diphenyl anthracene, and rubrene from Acros Organics B.V.B.A., and palladium(II) octabutoxyphthalocyanine were purchased from Frontier Scientific.

For the photo-redox reaction, a Thorlabs M680L4 680 nm mounted LED was used. 1-Trifluoromethyl-3,3-dimethyl-1,2-benziodoxole was purchased from TCI and 1-phenylpyrolle and α, α, α-trifluorotoluene was purchased from Sigma-Aldrich

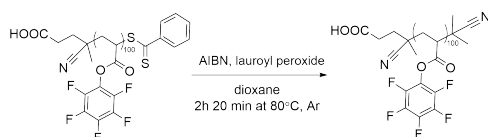### 3.3.2. Poly(pentafluorophenyl actrylate) (C)
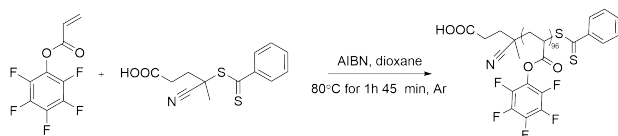
A dry 50 mL schlenk roundbottom flask with septum was loaded with pentafluorophenylacrylate **A** (2.0006 g, 8.402 mmol, 143 eq.) and, dissolved in 2 mL of 1,4-dioxane (anhydrous, Sigma-Aldrich), 4-cyano-4-(phenylcarbonothioylthio)pentanoic acid **B** (16.4 mg 58.7 µmol, 0.1 eq., Sigma-Adrich) and azobisisobutyronitrile (0.967 mg, 5.89 µmol, 0.1 eq.). The solution was degassed for 45 min and reacted under argon in an 80°C oilbath while conversion was checked with ^{19}F NMR. After 1h and 45 min reaction was quenched by submergence in liquid nitrogen. Oxygen was let in while the reaction mixture melted.

The reaction product was dissolved in 5 mL of dichloromethane and precipitated in cold pentane. The reaction product was filtered using a glass filter under vacuum and washed 3 times with 5 mL pentane. Residual solvent was evaporated off under reduced pressure, precipitated, and dried under reduced pressure again yielding a fluffy pink powder (865 mg, 37.4 µmol, 43%).

^{1}H NMR (400 MHz, CDCl$_3$): δ 3.09 (br, 1H), 2.50 (br, 2H), 2.60-1.86 (br, 2H) ppm. **^{19}F NMR** (376 MHz, CDCl$_3$): δ -153.23 (br, 2F), -156.76 (br, 1F), -162.17 (br, 2F) ppm. **SEC** (THF): Đ = 1.2, $M_{w,app}$ = 19 kg/mol. **IR** (neat): 1783 (m), 1516 (s), 1082 (m), 990 (s).

3.3.3. End-cap modification of poly(pentafluorophenyl acrylate) (D)

Poly(pentafluorophenyl acrylate) **C** (867.5 mg, 37.5 µmol, 1 eq.), azodiisobutyronitrile (122.2 mg, 744 µmol, 20 eq.), and lauroyl peroxide (29.737 mg, 74.6 µmol, 2 eq.) were dissolved in 10 mL of 1,4-dioxane (anhydrous, Sigma-Aldrich) and transfered in a dry 50 mL schlenk roundbottom flask with septum. The solution was degassed for 1 h and 50 min, and subsequently heated in an 80 °C oilbath for 2 h and 20 min. The reaction was terminated by quenching in liquid nitrogen and opening the schlenk flask to let oxygen in.

The solution was transferred to a 50 mL round-bottom flask and the schlenk was washed 3 times with 1 mL of dichloromethane. Next, the solution was dried under reduced pressure and precipitated and dried, using the method described above with 2 mL DCM to dissolve, 3 times. The product was a white fluffy powder (502.5 mg, 21.8 µmol, 58%).

^{1}H NMR (400 MHz, CDCl$_3$): δ 3.08 (br, 1H), 2.49 (br, 2H), 2.62-1.85 (br, 2H) ppm. **^{19}F NMR** (376 MHz, CDCl$_3$): δ -153.22 (br, 2F), -156.75 (br, 1F), -162.17 (br, 2F) ppm. **SEC** (THF): Đ = 1.2, M_w = 19 kg/mol.

3.3.4. Polymer P1

Under inert conditions, poly(pentafluorophenyl acrylate) **D** (150.2 mg, 6,51 µmol, 1 eq.) and dodecyl amine (22.944 mg, 124 µmol, 19 eq.) were dissolved in 5 mL of dry THF and loaded in a dry Schlenk tube with screw cap. Reaction was heated under argon in a 50°C oilbath for 22 h (conversion was checked with ^{19}F NMR).

^{19}F NMR (376 MHz, CDCl$_3$): δ -153.21 (br, 2F), -156.89 (br, 1F), -162.25 (br, 2F),-163.48 (d, 2F), -165.05 (t, 2F), -170.87 (t, 1F) ppm.

Jeffamine (1.2971 g, 1.24 mmol, 191 eq.) was dried in a 50°C oven with phosphorus pentoxide as a drying agent overnight and added to the reaction mixture. The mixture was heated, under argon, in a 50°C oil bath for 5 h.

The reaction product was purified by dialysis (6-8 kDa membrane) for 48 h in THF and 48 h in methanol replacing solvent every 24 h. Next, the product was dried under reduced pressure, and in a vacuum oven, to yield a waxy polymer end product (278.2 mg, 3.19 μmol, 49%).

^{1}H NMR (400 MHz, CDCl$_3$): δ 6.25 (br, 2H), 3.84- 3.44 (m, 2H), 3.38 (s, 3H), 1.89 (s, 2H), 1.26 (s, 2H), 1.13 (s, 3H), 0.88 (t, J = 6.8 Hz, 3H) ppm. **FT-IR** (neat): 2865 cm^{-1} (m), 1092 cm^{-1} (s). **SEC** (DMF): $Đ$ = 1.2, $M_w = 36$ kg/mol. **SEC** (PBS): $Đ$ = 1.4, $M_w = 25$ kg/mol.

3.3.5. Polymer P2

P2 was prepared using the same procedure as **P1** with 150.0 mg (6.51 μmol, 1 eq.) poly(pentafluorophenyl acrylate) **D**, 34.380 mg (185 μmol, 29 eq.) dodecyl amine and 1127.4 mg (1.08 mmol, 166 eq.) of Jeffamine yielding 240.0 mg (3.1 μmol, 48%) isolated end product.

After dodecyl substitution: **^{19}F NMR** (376 MHz, CDCl$_3$): δ -153.32 (br, 2F), -157.39 (br, 1F), -162.60 (br, 2F),-163.68 (d, 2F), -165.45 (t, 2F), -171.39 (t, 1F) ppm. Final Product: **^{1}H NMR** (400 MHz, CDCl$_3$): 6.30 (br, 1H), 3.84- 3.43 (m, 2H), 3.38 (s, 3H), 1.87 (s, 2H), 1.26 (s, 2H), 1.13 (s, 3H), 0.88 (t, J = 8.5 Hz 3H) ppm. **FT-IR** (neat): 2865 cm^{-1} (m), 1092 cm^{-1} (s). **SEC** (DMF): $Đ$ = 1.2, $M_w = 33$ kg/mol. **SEC** (PBS): $Đ$ = 1.4, $M_w = 34$ kg/mol.

3.3.6. Polymer P3

P3 was prepared using the same procedure as **P1** with 150.2 mg (6.51 μmol, 1 eq.) poly(pentafluorophenyl acrylate) **D**, 45.836 mg (247 μmol, 38 eq.) dodecyl amine, and 967.5 mg (0.93 mmol, 143 eq.,) of Jeffamine yielding 299.6 mg (4.42 μmol, 68%) isolated endproduct.

After dodecyl substitution: **^{19}F NMR** (376 MHz, CDCl$_3$): δ -153.31 (br, 2F), -157.49 (br, 1F), -162.69 (br, 2F),-163.67 (d, 2F), -165.51 (t, 2F), -171.46 (t, 1F) ppm. Final Product: **^{1}H NMR** (400 MHz, CDCl$_3$): 6.34 (br, 1H), 3.8- (s, 2H), 3.38 (s, 3H), 1.83 (s, 2H), 1.27 (s, 2H), 1.14 (s, 3H), 0.88 (t, J = 6.7 Hz, 3H) ppm. **FT-IR** (neat): 2865 cm^{-1} (m), 1092 cm^{-1} (s). **SEC** (DMF): $Đ$ = 1.3, $M_w = 34$ kg/mol. **SEC** (PBS): $Đ$ = 1.6, $M_w = 34$ kg/mol.

4. Chromophores

In this section, the optical properties, as well as the stability of the used chromophores are briefly discussed. Here, three upconversion pairs are used which give access to three regions of wavelengths of the upconverted light. Therefore the system can be tuned by dissolving different upconversion pairs inside the polymer matching with the requirements of photocatalyst or reaction products, which shows the universality of the approach.

4.1. Upconversion pair 1

Upconversion pair 1 consist of a sensitizer (**S1**) platinum octaethylporphyrin (PtOEP) and an emitter (**E1**) diphenylanthracene (DPA). The chemical structure of **S1** and **E1** is depicted in Figure 4.1.

Sensitizer
PtOEP

Emitter
DPA
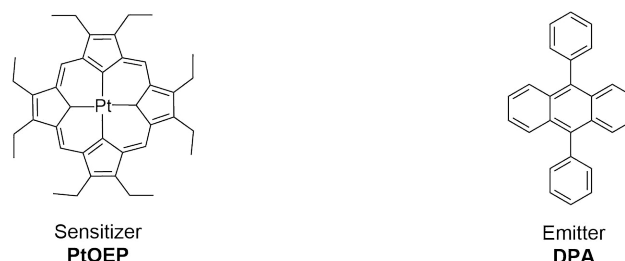
Figure 4.1.: Upconversion pair 1 (**S1 E1** resp.)

S1 is a red crystalline solid that can be dissolved in chloroform to make a pink solution (see FigureA.18) whereas **E1** is a white powder and, dissolved in chloroform (Figure A.18), will create a colourless transparent solution. When **E1** is illuminated with UV-light, it emits blue light. The normalized absorbance and fluorescence spectra of **S1** and **E1** are shown in Figure 4.2. The absorbance of **S1** has its maxima at 382 nm and 536 nm, it emits at a wavelength of 646 nm, although low in intensity. **E2** absorbs between 350-400 nm with maxima at 357 nm, 376 nm, and 397 nm. The intensity of the fluorescence of **E1** is much higher than **S1**, and has a maximum at 412 nm and 429 nm (blue, as observed).
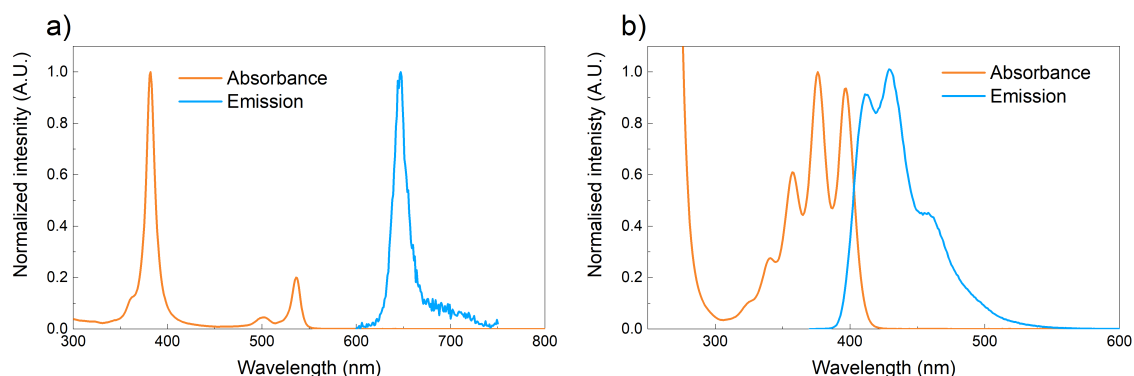

Figure 4.2.: Normalized absorbance and photo luminescent emission spectra of a) **S1** and b) **E1** ($c = 7.45\,\mu M$ and $31.0\,\mu M$ and $\lambda_{ex} = 380$ nm and 360 nm respectively.

4.2. Upconversion pair 2

Upconverison pair 2 (see Figure 4.3) were synthesised previously by Van Vliet.[7] The sensitizer, platinum (tetraphenyltetranaphtho[2,3]porphyrin (**S2**), is a green crystaline compound, which gives a bright green solution when dissolved (Figure A.18). The emitter 2,5,8,11-tetra-tert-butylperylene (**E2**), is a yellow powder, which also gives a yellow solution.
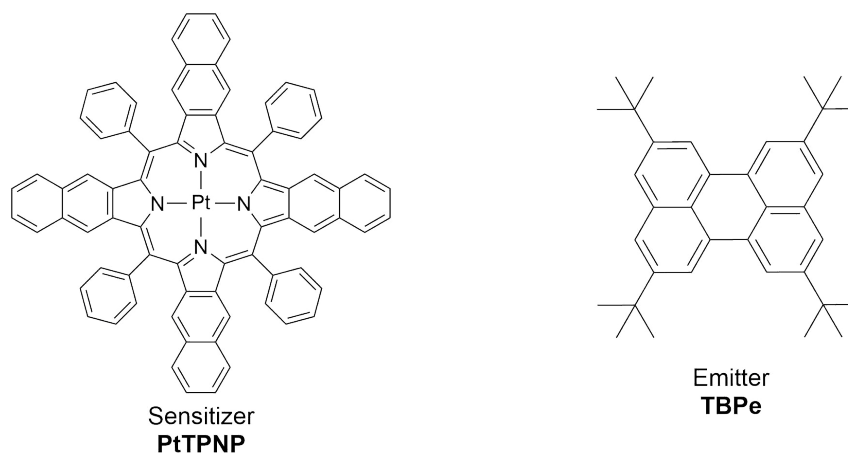
Sensitizer
PtTPNP

Emitter
TBPe

Figure 4.3.: Upconversion pair 2 (**S2 E2** resp.)

The normalized absorbance and fluorescence spectra of **S2** and **E2**, given in Figure 4.4, shows an absorbance peak for **S2** at 690 nm. **E2** absorbs around 400-450 nm with its maximum at 440 nm. The fluorescence of **S2** could not be measured at an excitation wavelength of 436 nm. Exciting the sensitizer at its absorbance maximum could have resulted in a signal, nevertheless, this measurement was not performed. The emission of **E2** lies between 450 nm and 500 nm, and shows a maximum at 461 nm. Hence emitting in the blue/green region.
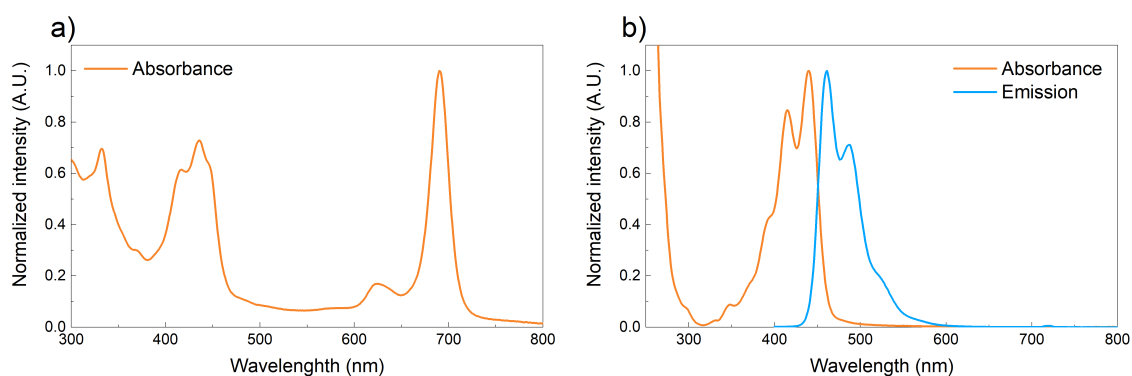
Figure 4.4.: Normalized absorbance and photo luminescent emission spectra of a) **S2** and b) **E2** ($c = 7.45\,\mu$M and $31.0\,\mu$M respectively and $\lambda_{ex} = 360$ nm).

4.3. Upconversion pair 3

The last upconversion pair used in this project uses palladium(II) octabutoxyphthalocyanine (PdPc, **S3**) as sensitizer, and rubrene (**E3**) as emitter (see Figure 4.5). **S3** has a deep green colour and dissolves to give a bright green solution. **E3** is a red solid and gives very bright orange solutions when dissolved (see FigureA.18).
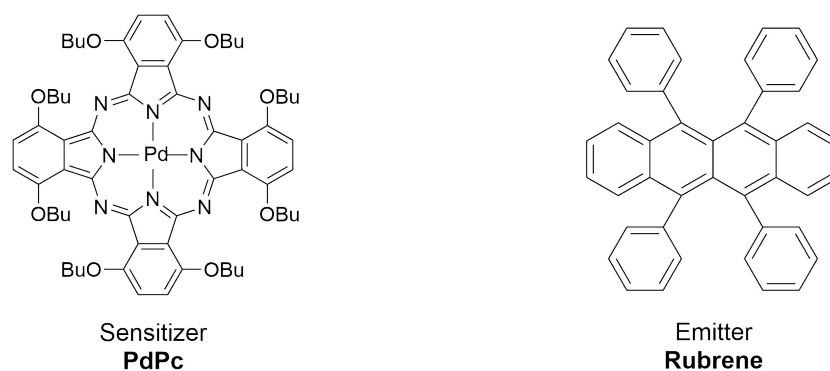
Figure 4.5.: Upconversion pair 2 (**S2 E2** resp.)

The absorbance spectrum of **S3** (Figure 4.6 a)) shows a maximum at 735 nm and a maximum emission at 758 nm. Figure 4.6 b) shows high absorbance for **E3** at 450-550 nm, with maxima at 494 and 529 nm. The fluorescence spectrum shows an emission maximum at 558 nm hence emitting green light.
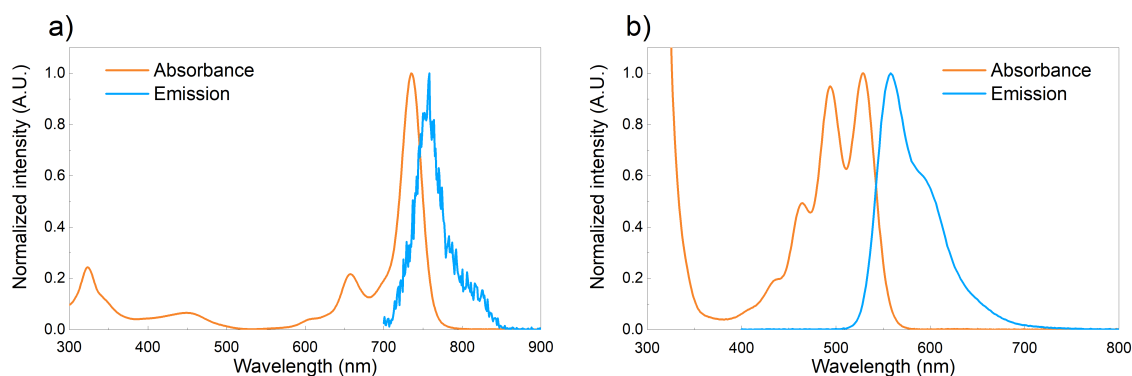

Figure 4.6.: Normalized absorbance and photo luminescent emission spectra of a) **S3** and b) **E3** ($c = 7.34\,\mu M$ and 31.0 μM and $\lambda_{ex} = 324$ nm and 316 nm respectively.

As can be concluded from the above discussion, all chromophores have their own absorbance and emission spectra with their own distinct maxima of excitation and fluorescence. For TTAUC, the sensitizer must be excited, hence an excitation wavelength λ_{ex} must be employed that is compatible with the absorbance spectra of the chromophores. As the emitter fluoresce the upconverted photons, the emission spectra of the pure emitter in solution give an indication at which wavelengths the upconversion pair together emits. In Table 4.1 the expected outcome of TTAUC with the upconversion pairs is given. Although many factors could influence the actual emission spectrum in TTAUC the table can act as a first estimate.

Table 4.1.: Expected excitation wavelengths and emission wavelengths for TTAUC for the different upconversion systems based on the spectra of Figure 4.2-4.6.

Upconversion pair	required excitation wavelength	Expected emission
1	536 nm	400-450 nm
2	690 nm	450-500 nm
3	735 nm	550-600 nm

4.4. Heating and sonication resilience of chromophores

The sample preparation methods used in making the upconversion solutions (that will be discussed in chapter 5), could be harmful to the chromophores used. To find out if the chromophores can withstand the used methods, a control experiment was done in which the chromophores were placed in an 80°C oven for 45 min, in a sonication bath for 45 min, or stored in the dark. The results are given in Figure 4.7.

From the absorbance spectra of all chromophores except **E3**, no significant deviation from the control is observed indicating that both heating and sonication of the samples give rise to no serious degradation of the chromophores. The spectra of **E3** show, however, a decreased intensity in absorbance after sonication. Although, this could be a result of the severe vibrations in the bath, the degradation could also be a result of the fact that during sonication the emitter was not protected against the light. It is known that rubrene tends to undergo photo-oxidation reactions, giving a colorless oxidation product.[36] Therefore, it is also deemed possible, that during sonication, the rubrene has been oxidized as the other 2 methods were kept dark the whole time and did not show a decreased absorbance spectrum. A control experiment of sonication in the dark should show if the photo-oxidation took place, or that **E3** is degrading during the sonication. Either way, it can be concluded that **E3** is a sensitive molecule and should be kept dark as much as possible.
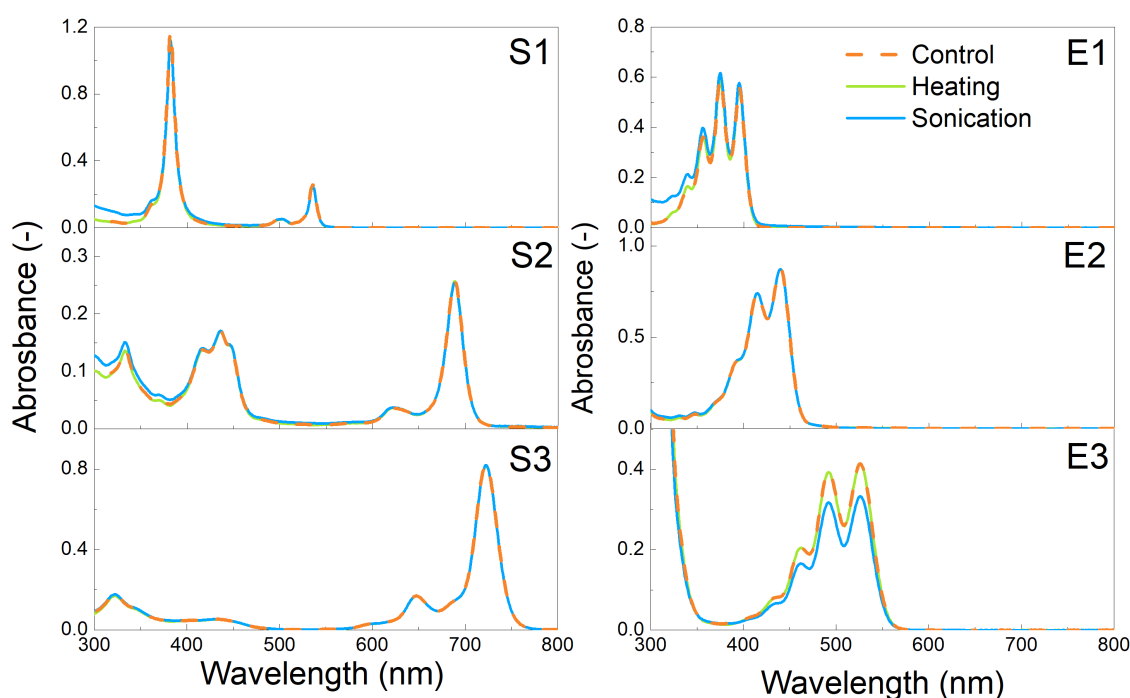

Figure 4.7.: Absorbance spectra of the chromophores placed in a 80°C oven (heating), a sonication bath (sonication) or in a fume hood wrapped in aluminum foil (control). ($c(S1) = 4.17\,\mu$M, the rest of the sensitizers and emitters have $c = 5.00\,\mu$M and 50.0 μM respectively.)

5. Up-conversion

This chapter gives an overview of the performed experiments concerning upconversion. First, the photoluminescence spectra of the upconversion pairs in organic solvents (chloroform) are discussed. Subsequently, different sample preparation methods were investigated to see if a homogeneous solution could be made to minimize scattering and attenuation of the light in the solution and maximize the upconversion intensity. The stability of oxygen quenching is inspected by comparing control and degassed solutions with each other. Lastly, different ratios of chromophores and the influence of dilution on the upconversion in water are analyzed.

5.1. Upconversion in chloroform

In Figure 5.1, the upconversion spectra of a degassed solution with upconversion pair 1 and 2 in chloroform. Upconverion pair 3 was also measured, but did not show any signal when excited at 730 nm, a possible explanation for this is due to the spectroscopy machine that was used. This will be discussed in section 5.6. The spectra of **S1** and **E1** (Figure 5.1 a)) show maxima 414 nm and 434 nm which is in well agreement with the fluorescence spectra of Figure 4.2 b). The peak at 647 nm can be assigned to the fluorescence of **S1**. In Figure 5.1 b) the TTAUC spectrum of **S2** and **E2** show an emission maximum at 463 nm which also is consistent with the fluorescence measurements on the individual components (Figure 4.4 b)).
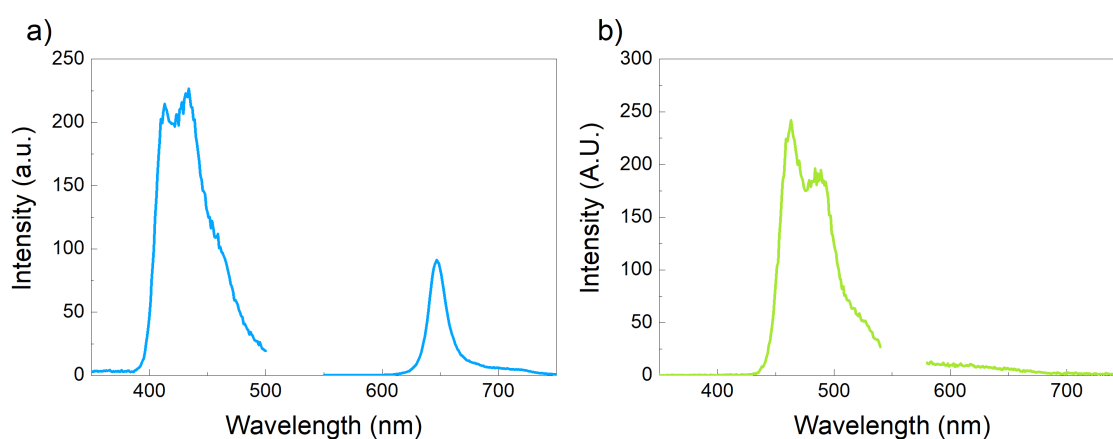

Figure 5.1.: Upconversion photoluminescence spectra of a) **S1** and **E1** and b) **S2** and **E2** in chloroform ($c = 5.0 \, \mu$M and 50 μM for sensitizer and emitter respectively, $\lambda_{ex} = 532$ nm and 560 nm for pair 1 and 2 respectively).

5.2. Sample preparation methods

In the work of Van Vliet[7], sensitizer and emitter together with an amphiphilic polymer were first dissolved in an organic solvent, the solvent was subsequently evaporated and the remaining molecules were re-dissolved in water. Utilizing this method with **S1**, **E1** and **P7** resulted in opaque, and poorly
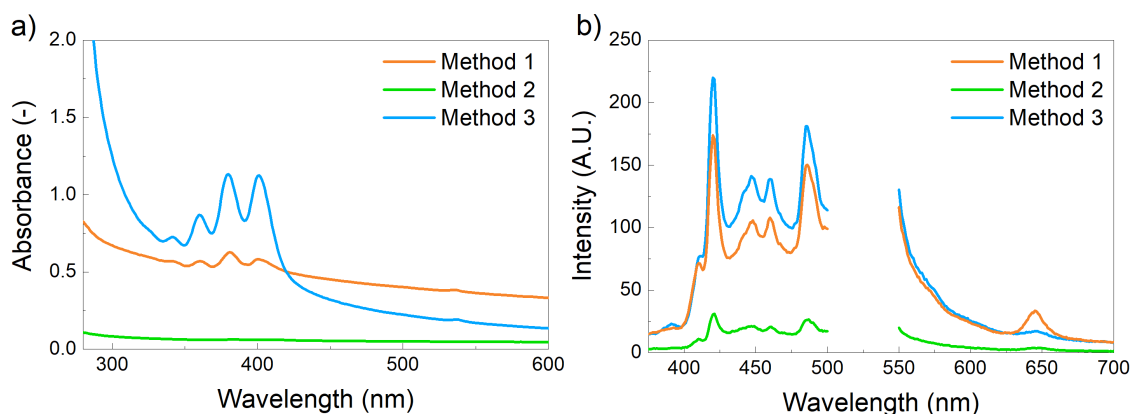
Figure 5.2.: a) Absorbance and b) photoluminescence spetra of the solutions prepared with the different sample preparation methods ($\lambda_{ex} = 532$ nm, $c = 5.00\,\mu$M, $0.500\,\mu$M for **P7** and **S1** respectively, for **E1** in method 1 and 2 $c = 100\,\mu$M and for method 3 $c = 99.4\,\mu$M)

dissolved mixtures. Because this introduces a lot of scattering and makes it difficult to know if the upconversion signal is coming from chromophores dissolved in the hydrophobic pocket of the polymer, a method should be devised which would make homogeneous dissolved solutions of polymer, emitter, and sensitizer.

Three methods were investigated to this end: method 1 involved dissolving the polymer, sensitizer, and emitter in chloroform, evaporating the chloroform off under N_2 flow, and dissolving it again in water. For methods 2 and 3 an aqueous polymer stock was made and the chromophores were dissolved in an organic solvent. The polymer stock was added to the chromophores and for method 2 the solvent was evaporated off by gentle heating. These experiments were done using **S1**, **E1**, and **P7**, and for method 2 and 3 chloroform and dioxane were used as solvents respectively. The absorbance and PL-spectra are shown in Figure 5.2 and a picture of the resulting solutions is given in Figure A.19. In this picture the solutions utilizing methods 1 and 3 show to be turbid while the solution prepared, by method 2, is clear. Although this would indicate that method 2 would be better in dissolving the molecules, however, the absorbance and emission spectra hardly show any signal. This could be explained as S1 precipitation could clearly be distinguished around the stirring bean in the sample. This indicates that very little chromophore was dissolved in the polymer, and all was stuck to the stirring bean. The sample made with method 1 was somewhat more opaque than the sample prepared by method 3, this is in agreement with the spectra of Figure 5.2 a) as method 1 shows more scattering signal. From the upconversion spectra of Figure 5.2, it can also be seen that method 3 gave, not only visually the best solution, but also shows a stronger absorbance signal with less scattering and more upconversion signal. This could be a result of the use of a water-soluble solvent.

The upconversion spectrum of Figure 5.2 b) shows to be dissimilar to the spectrum measured in chloroform (5.1 a)). It is uncertain what causes the spectrum to look this erratic, with peaks at 420 nm and 486 nm that are not found in the chloroform spectrum. Also, in the literature, no case was found that could explain the peaks observed.

To test whether the observation that a water-soluble solvent would result in a higher upconversion intensity is more generally valid, multiple solvents were tried, to dissolve the chromophores. The solvents were chosen to have a low boiling point such that they could be evaporated easily, which would be necessary for biological/green applications. The solvents chosen for this are the water-soluble solvents: THF and acetone, the water-insoluble solvents: chloroform, benzene, and DCM, and one solution was made without the use of a solvent. Because as little solvent as possible should be in

the final solution, the solvent was evaporated by heating, as was done in method 2. The results are depicted in Figure 5.3. Firstly, it should be noted that despite being careful with the illumination of light on the chromophores, the samples of E3 lost color during the process highlighting the instability of E3. However, a general trend could be recognized that water-insoluble solvents gave solutions in which almost no chromophores could be dissolved. The solvent also formed a bubble around the stirring bean (see Figure A.20 c)-e)), so it is possible that all chromophore ended up stuck to the stirring bean once more. Equivalently, the samples from which only polymer stock was added directly to the chromophores, also showed no signs that any chromophore was dissolved as many particles were floating around in the solution. The samples in which water-soluble solvents were used (1,2,7,8,13,14 in Figure 5.3) showed to be significantly better dissolved, here acetone showed the best solution in which very few particles could be recognized. The upconversion pair that showed to be giving the most homogenous and clear solutions was that of upconversion pair 2, for upconversion pairs 1 and 3 still some particles could be recognized in the solution.
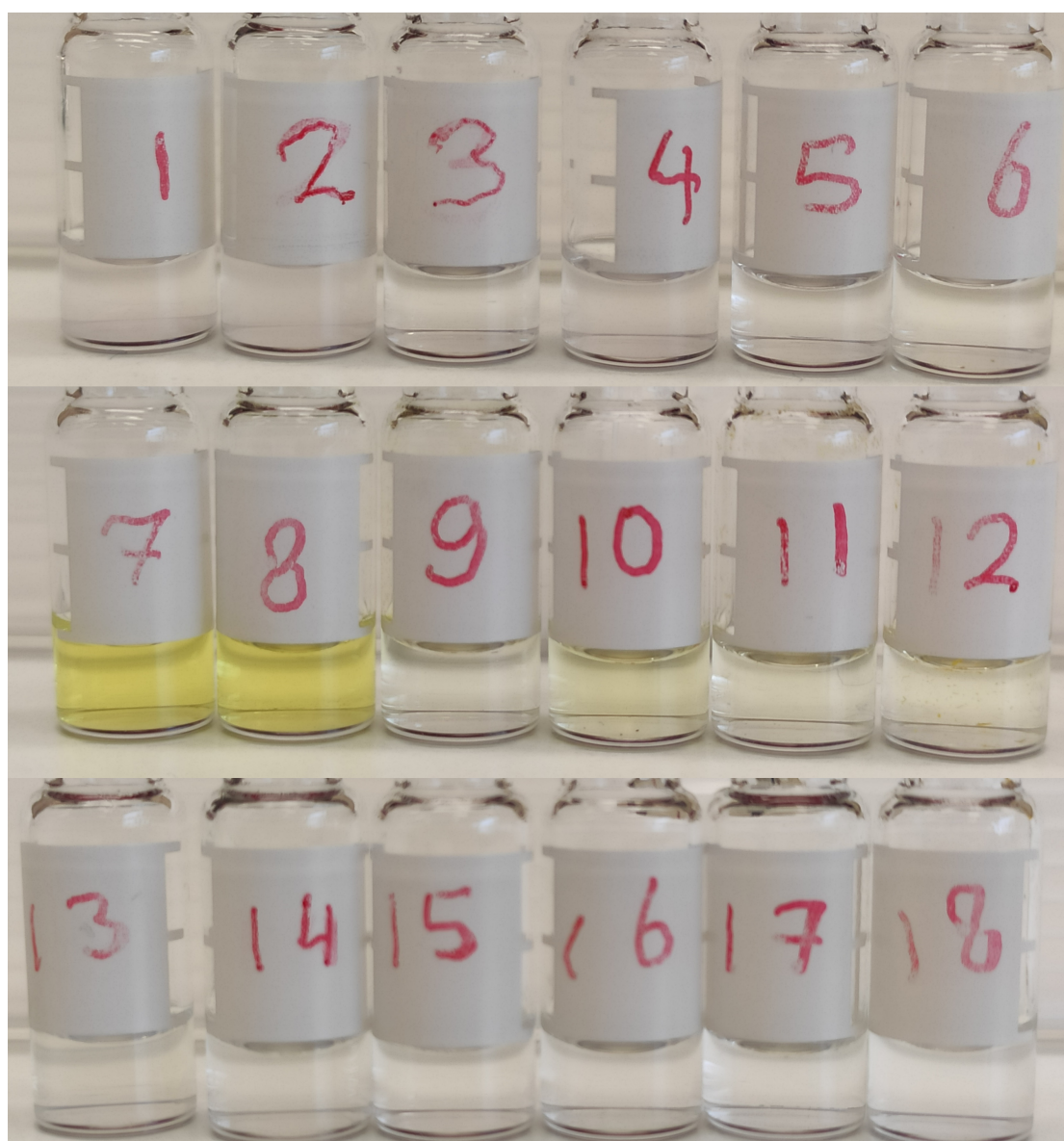

Figure 5.3.: Photographs of solutions prepared by dissolving chromophores in 50 μL of different solvents, before 0.5 mL of **P7** solution in water ($c = 1$ mg/mL) was added to the samples. Sample 1-6: **S1 E1**, sample 7-12: **S2 E2**, Sample 13-18: **S3 E3**. Solvents added are FLTR: THF, acetone, chloroform, benzene, DCM, no solvent. (Ratio polymer:sensitizer:emitter = 1:0.1:20)

Checking how much of the organic solvent had evaporated during the heating was done with ^{1}H NMR in CD$_3$OD on sample 8 (for details see Figure A.21), from this measurement it follows that 97% of the acetone was evaporated during the process.

As acetone and upconversion pair 2 came out as the best to perform further experiments with, samples were prepared using method 2 with **P1-P6**, and **S2 E2** in acetone on which the particle sizes were determined with DLS (Figure 5.4). Comparing these measurements to the measurement of the polymer solution only (Figure 3.17) it is noted that the particles in solution are much larger after the addition of the chromophores (around 100 nm compared to 10 nm without upconversion pair 2). Therefore, it is concluded that aggregates form when the chromophores are added to the solution. Control experiments with solutions without **S2** and **E2** and without polymer show that the chromophores tend to aggregate with each other (Figure A.22). Therefore, the measured aggregates in the results of Figure 5.4 are possibly originating from the chromophores only, and not the polymers.

In this section, different sample preparation methods were investigated. From UV-vis and upconversion spectra of the resulting solutions, it was concluded that adding chromophores dissolved in a water-soluble solvent gave somewhat higher upconversion intensity, absorbance, and less scattering in solution. When trying different solvents the use of acetone proved to be superior in comparison with other solvents and therefore, further experiments were done using this solvent. DLS measurements, however, showed aggregation in the solution which was attributed to the presence of the chromophores in the solution. A final control experiment, measuring the upconversion in solution made using the described method with and without polymer, should give a decisive result on whether the polymers improve the upconversion, or if the acetone dissolves the chromophores and enables a pathway for upconversion and no polymer is needed. Furthermore, it should be noted that no significant difference between the polymers was measured with different ratios of dodecyl to Jeffamine grafts in the polymer, however, more experiments should be done to conclude if there is in general no difference in the polymer. For example, measuring the upconversion spectra of chromophores dissolved in all the different polymers.
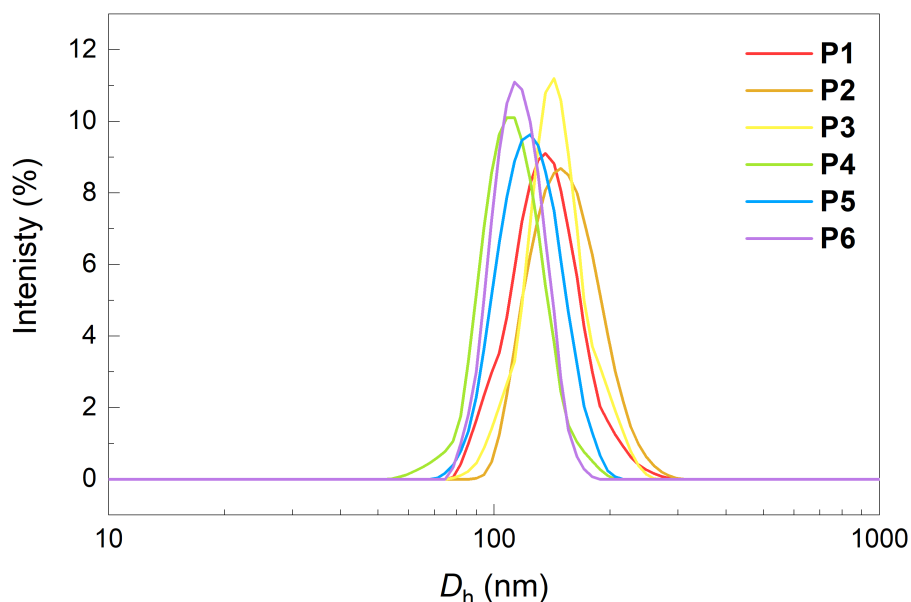

Figure 5.4.: Size distribution of **P1-P6** in water ($c = 1$ mg/mL) with upconversion pair 2 dissolved in acetone added to the polymer (polymer:**S2**:**E2** = 1:2:40)

5.3. Influence of oxygen on upconversion

Solutions of polymer and chromophores were made on which the influence of degassing the solution was measured. Noteworthy was the color change of the rubrene after water was added to the chromophore acetone solution. The color changed instantly from bright orange to pink, (compare the color **E3** of Figure A.18 with Figure A.23). Possibly the solution forms excimers or exciplexes upon the addition of the water which absorbs the light at a different wavelength. The results of upconversion pairs 1, 2, and 3 are given in Figure 5.5 a, b and c respectively. All spectra show behavior that is characterized by many peaks which are not in accordance with Figure 5.1 and literature[2,37]. The PL spectrum of Figure 5.5a shows, however, the same peaks as 5.2b. And therefore, although not as expected, the results are reproducible and therefore will be used for analysis.

From the spectra of Figure 5.5, the upconversion intensity is approximately the same and even slightly decreased after degassing for upconversion pairs 1 and 2. This is to be expected as oxygen quenching is reduced by removing the oxygen from the solution. Additionally, SCPNs are reported to act as a barrier against oxygen quenching itself[7], which could explain the slight decrease in upconversion intensity. However, the results of Figure 5.5c show that degassing leads to a nearly doubling of the upconversion intensity. A possible explanation could be that too much acetone was added which resulted in the chromophores being dissolved by the acetone and not in the hydrophobic pocket of the polymer, therefore this system does not have the protection against oxygen quenching of the SCPN. A control experiment using method 2 to evaporate the organic solvent should give more insight if this explanation is correct.
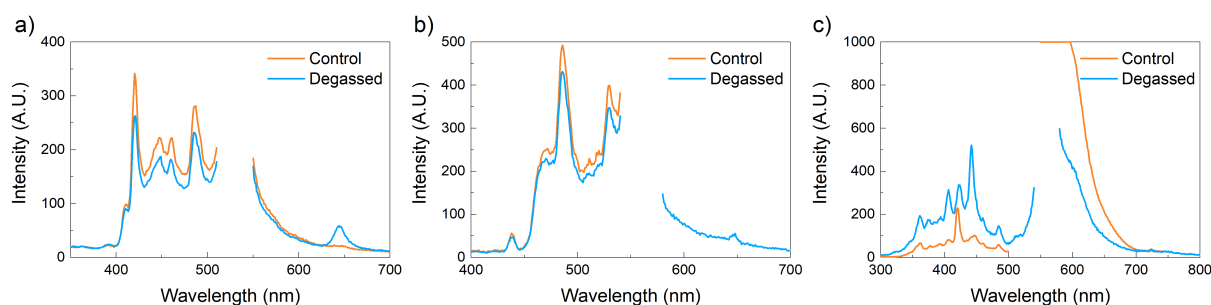

Figure 5.5.: Photoluminescence spectra of a) **P4 S1 E1** ($\lambda_{ex} = 532$ nm) b) **P5 S2 E2** ($\lambda_{ex} = 560$ nm) c) **P5 S3 E3** ($\lambda_{ex} = 532$ nm for control and $\lambda_{ex} = 560$ nm for degassed solution). Samples were prepared using method 3 with a 1 mg/mL polymer solution. polymer:sensitizer:emiter=1:0.2:44, 1:0.2:40, and 1:0.2:33 for a), b), and c) respectively.

5.4. Sensitizer to emitter ratio

As discussed in section 2.6, the backward energy transfer from the T_1 state of the emitter to the T_1 state of the sensitizer is reduced when the emitter to sensitizer ratio is increased. To inspect phenomena, two ratios of sensitizer: emitter are investigated, the results are given in Figure 5.6 a). In the figure, a small decrease in PL intensity can be distinguished which makes the 1:0.1:20 a better ratio of polymer:sensitizer:emitter. In the experiments of 5.4 a ratio of 1:2:40 was used, and although no PL measurements were done on these samples, there was visual evidence that the DP = 200 polymers (**P4**-**P6**) resulted in better, homogenously dissolved solutions than the slightly opaque solutions made with **P1**-**P3** (see Figure A.24). This is a result of **P1**-**P3** having a smaller molecular mass, and therefore, there was, in mass, more sensitizer and emitter added to **P1**-**P3** than the heavier **P4**-**P6**. It is evident that trying to maintain a fixed molar ratio of polymer:sensitizer:emitter results in lower concentrations of chromophores in the larger polymers as the cumulative size of the hydrophobic pocket of the SCPN in a 1 mg/mL polymer solution would approximately be equal for both solutions. Therefore dissolving
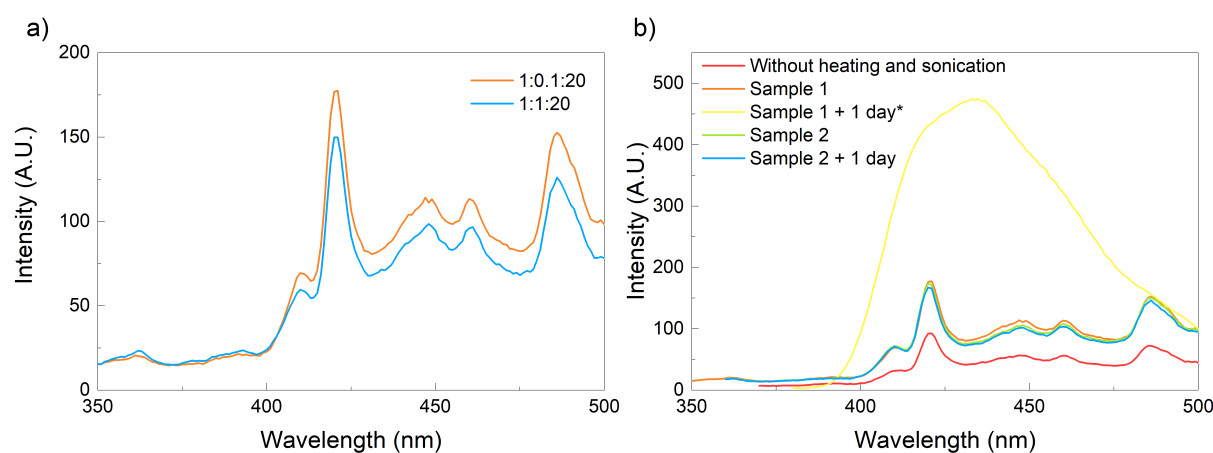
Figure 5.6.: Upconversion PL spectrum of **P7** ($c = 5\,\mu\text{M}$), **S1**, and **E1** prepared using method 1 a) with different ratio's of polymer:sentitizer:emitter ($\lambda_{ex} = 532\text{nm}$) b) comparing different samples made on different days, and the repeating the measurement after 1 day. ($\lambda_{ex} = 532\text{nm}$, **P7:S1:E1** = 1:0.1:20.) *Measurement was done with a lower excitation light intensity (600 V)

a fixed molar ratio of chromophores to polymer is not recommended. An optimum value of the ratio between polymer, sensitizer, and emitter has not been found, however, it is recommended to lower the overall concentration of the chromophores to reduce the aggregation as seen in Figure 5.4, possibly the hydrophobic pockets of the SCPN are already saturated with sensitizer and emitter resulting in the aggregation of the residual chromophore that remained in the water phase of the solution. Therefore, further research is recommended.

5.5. Short term stability and reproducibility

Finally, the spectra of multiple samples made at different times were compared to analyze the reproducibility of the upconversion measurements (Figure 5.6b). The spectra of all samples look similar except for the measurement done after one day on sample 1. This spectrum does not show the irregular behavior of the others and shows many similarities with the spectrum made in chloroform (5.1a) and found in the literature using other encapsulation approaches.[37] However, it was only measured once on two samples prepared and measured on the same day. No explanation of the phenomenon was found and therefore, a way should be found to reproduce these results. The other spectra have the same characteristics and comparing the two measurements on sample 2 no significant degradation is observed after one day.

5.6. A note on spectrometers

In this project, multiple fluorescence spectrometers have been used to measure the fluorescence, and TTAUC PL spectra of various solutions. Two Aligent, Cary Eclipse spectrophotometers (a new and an old machine) and a spectrometer from Edinburgh Instruments were used. To decide which machine would be used for the project, a measurement was done on all spectrometers, as depicted in Figure 5.7 a). A very high noise was measured with the Edinburgh Instruments apparatus, here the signal nearly could not be distinguished from the noise. A better signal was received from the Cary eclipse machines, here the new device showed a smoother curve and therefore this machine was chosen to conduct the measurements with.

However, in the course of the project, peculiar features of this machine were discovered. First of all, unexpected peaks were measured or no upconversion could be measured for the wavelengths specified
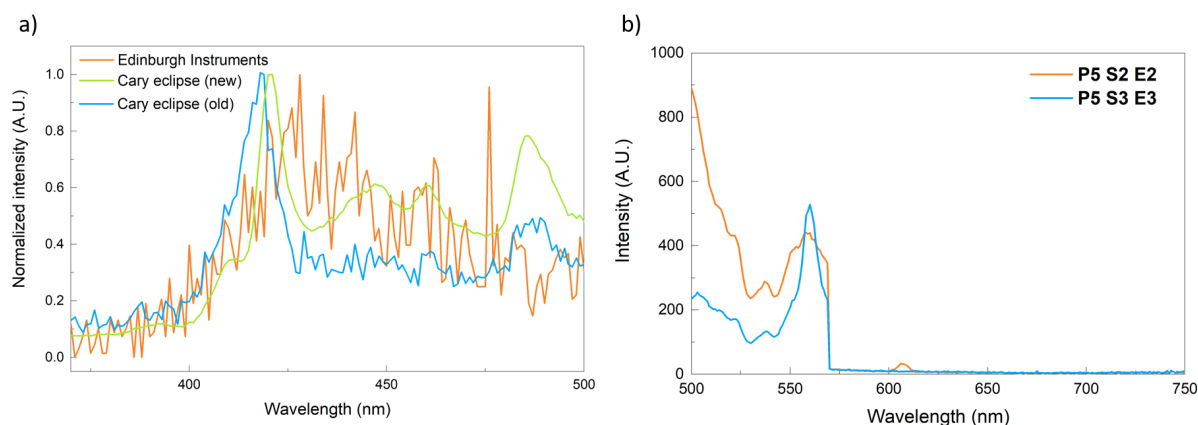
Figure 5.7.: a) TTAUC PL spectra of a solution of **P7**, **S1** and **E1** (prepared with method 1, $c = 5\,\mu M$, 0.5 μM, and 100μM respectively). b) Excitation scan of the degassed solutions of Figure 5.5 b) and c) ($\lambda_{em} = 486$ nm and 442 nm respectively).

in the literature of upconversion pairs 2 and 3 (690 nm and 730 nm) respectively).[2,37]. It was assumed that the upconversion intensity was too low, or non-existent, and therefore no signal could be measured. However, when performing an excitation scan on the samples a cut-off at 730 nm was observed from which the upconversion signal abruptly jumped to zero (see Figure 5.7). This was measured on both Cary eclipse machines, on multiple samples, and different days. The only possible explanation found for this behavior is the settings of the excitation and emission filters that were set to automatic for all measurements. As fluorescence is usually measured by excitation by a low wavelength and measuring of higher wavelengths it could be the case that automatic filter selection will not let lower wavelengths pass to the detector resulting in the spectra of Figures 5.5 and 5.6. To check whether the cut-off was a characteristic of the machine, a measurement of the degassed **P5 S2 E2**, and **P5 S3 E3** was performed on the Edinburgh Instruments spectrometer. The results are given in Figure 5.8, here, although with noise, the upconversion spectra of upconversion pairs 2 and 3 are visible. The peaks around 480 nm for upconversion pair 1 and 550 nm for upconversion pair 2 are in agreement with the expected emission from Table 4.1. Therefore, it has become clear that without knowing what causes the Cary eclipse spectrometers to give no upconversion signal after 570 nm, the machine should not be used for upconversion PL measurements, and instead, the Edingburgh Instruments spectrometer could be used.
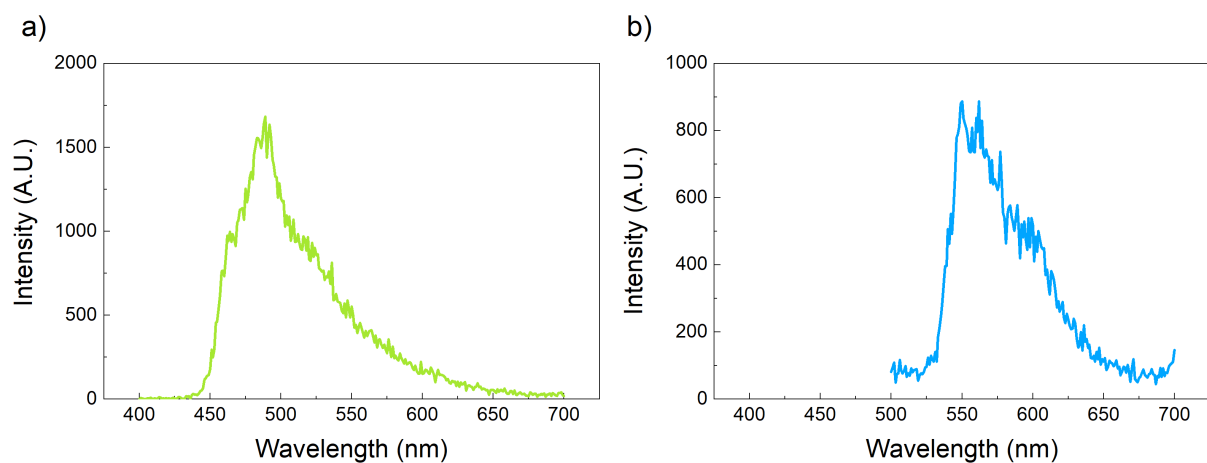

Figure 5.8.: TTAUC PL spectra of the solutions of Figure 5.5 b) and c) measured on the Edinburgh Instruments spectrometer ($\lambda_{ex} = 690$ nm and 730 nm respectively)

5.7. Experimental

Method 1: Polymer, sensitizer, and emitters were dissolved in chloroform. The required amount of compounds was transferred to a vial, subsequently, the chloroform was evaporated by an N_2 flow and placed in a vacuum oven of 50 °C for 3 hours. Water was added and the precipitated chemicals were dissolved by sonication and subsequently heated in an 80°C oven for 45 min.

Method 2: A polymer stock was made by dissolving the required amount of polymer in water, followed by sonication of the solution and heating in an 80°C oven for 45 min each. Leaving it to cool overnight. Sensitizer and emitter were dissolved in the required solvent and the polymer stock was added. The vial containing the chromophores and polymer was wrapped in aluminum foil and placed in an 80°C oil bath for 1 h, while stirring.

Method 3: A polymer stock was made using the description of method 2. Sensitizer and emitter were dissolved in the required solvent and polymer solution was added.

6. Photo-redox catalysis

As the goal of this project is to use TTAUC for photo-catalysis, an experiment was conducted in which the trifluoromethylation photocatalytic reaction as shown in Figure 6.1 was performed as reported by Eisenreich and Palmans.[33] In this reaction a solution was made of a pyrrole substrate (**A**), Togni reagent I (**B**), **S2**, **E2**, **P7** and N-phenylphenothiazine (PTH), the photocatalyst (see Figure A.25). The major and minor reaction products are given by the monosubstituted and disubstituted products (**H** and **I**) respectively. A 680 nm LED was available to perform the reaction with. Therefore, upconversion pair 2 was chosen as **S2** has an absorption maximum at 690 nm (section 4.2). To estimate if the upconverted light has enough energy for the reaction the expected energy of the upconverted photons (450-500 nm = 2.8-2.5 eV Table 4.1) was compared to the redox potential of PTH ($E_{1/2} = -2.1V$). Assuming that the reaction is a single electron process, meaning that the energy to excite the PTH should be at least 2.1 eV. Thus it was concluded that on a theoretical basis, the reaction should occur. The reaction would not occur with the LED wavelength of 680 nm as this corresponds to an energy of 1.8 eV.
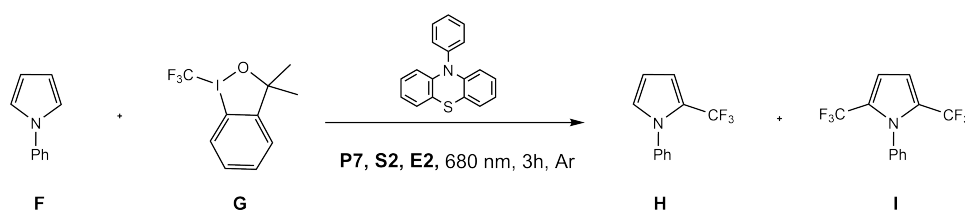
Figure 6.1.: Reaction equation of photocatalytic reaction that was performed with the utilisation of upconversion pair 2 and a 680 nm LED.

The trifluoromethylation reaction is easily checked by ^{19}F NMR as the starting compound has another shift than the end product ($\delta = 40$ ppm[38] and 55.97 ppm respectively). With an internal standard (being trifluoro toluene $\delta = 62.75$ ppm) the conversion can be determined. The results are depicted in Figure 6.2. Here the monosubstituted main product is identified, and there is also still starting compound left. From the internal standard, the conversion of the Togni reagent is 98%. However, the trifluoro methylated product of the reaction is only found to be only 1%. Effectively, this means that 97% of the fluorine could not be traced back in the spectrum. This could be a result of trifluoromethyl radicals terminating with each other to give hexafluoroethane or trifluoromethane which are gasses, and cannot be traced back into the NMR. To rule out the possibility of fluorine being left in the aqueous layer after extraction, an ^{19}F NMR of the aqueous layer (in water-d$_2$) was made (see Figure A.26). Here two peaks can be seen at $\delta = $ -129.90 -148.81 ppm, which have a very different chemical shift than in Figure 6.2, but due to different solvents, it could be that these peaks are representing the missing fluorine. This could be checked by measuring the ^{19}F NMR in D$_2$O of the begin and end product **G** and **H**.

Although this experiment showed to be very inefficient for the product formation, this experiment has shown that, using light that in theory could not initiate a reaction, still some product is formed during the reaction. However, without control experiments, it is too early to tell if the TTAUC was responsible for this. Experiments with and without chromophores should give more conclusive results.
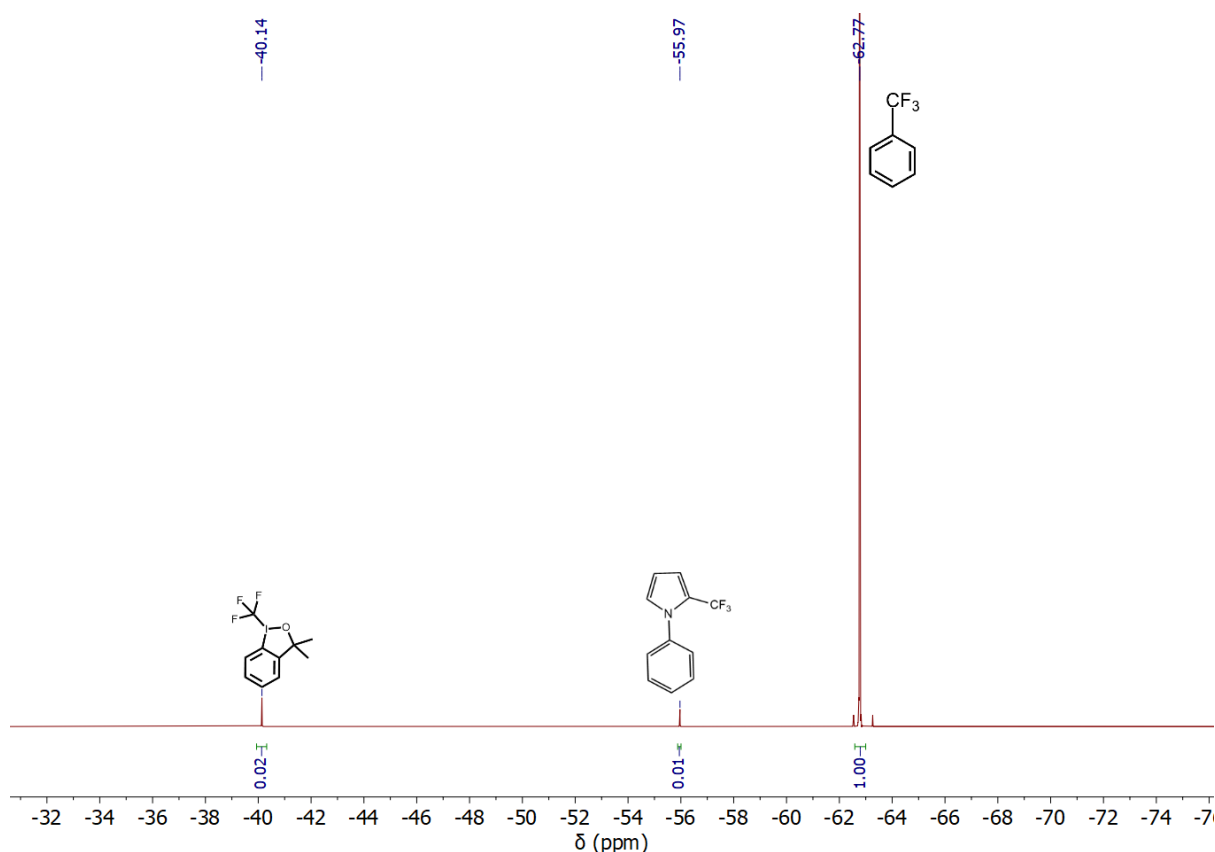
Figure 6.2.: ^{19}F NMR (376 MHz CDCl$_3$

6.1. Experimental

A 1.5 mL vial with septum screw cap was loaded with Togni reagent I (9.582 mg, 29.0 μmol, 1 eq.), 1-phenylpyrrole (6.442 mg, 45.0 μmol, 1.5 eq.), **P7** (9.829 mg, 0.106 μmol, 0.004 eq.), and N-phenylthiazine (0.195 mg, 0.70 μmol, 0.02 eq.). In another vial 200 μL acetone and 500 μL water was added to **S2** (0.175 mg, 0.145 μmol, 0.005 eq.) and **E2** (10.00 mg, 18.8 μmol, 0.65 eq.). This was transfered to the vial with reagents degassed for 5 minutes. Under nitrogen flow for cooling a 680 nm LED was shined on the sample at high intensity for 3 hours. Trifluorotoluene (6.68 μL, 1 eq.) was added to the sample and the solution was extracted three times with 0.5 mL chloroform-d$_1$. ^{19}F NMR was taken to check conversion.

^{19}**F NMR** (376 MHz, CDCl$_3$): δ -40.14 (s, 3F), -55.97 (s, 3F), -62.77 (s,3F) ppm.

7. Conclusion

In this project, the possibility of enabling TTAUC in water by solvation of the sensitizers and emitters in the hydrophobic pocket of SCPNs for photocatalysis in aqueous media is investigated. To this end, different amphiphilic polymers, with DP = 100, DP = 200, and different ratios of hydrophobic to hydrophilic side groups, were synthesized and characterized. From DLS measurements, it was shown that the polymers indeed formed nanoparticles with a hydrodynamic diameter of around 10 nm.

Furthermore, 3 pairs of sensitizers and emitters were characterized by their absorbance and fluorescence spectra, and from this, a prediction was made at which wavelengths the upconverted light is expected to be emitted. After the basic properties of the chromophores were investigated, several experiments were conducted to understand the behavior of TTAUC in an aqueous medium. First, a reference measurement was done on chloroform, however, the upconversion spectra could not be measured for all chromophores with the excitation wavelength found in literature or predicted from the absorbance spectra of the sensitizers. This was probably a result of the spectrometer that was used.

The main part of this research was concerned with optimizing a sample preparation method in which sensitizer, emitter, and the polymer formed a homogeneously dissolved, transparent solution. This is required to ascertain that the chromophores were dissolved inside the hydrophobic pockets of the SCPNs. Therefore, three sample preparation methods were compared, in which all particles were dissolved in an organic solvent, the solvent was subsequently evaporated and water was added. This resulted in opaque poorly dissolved solutions, furthermore, this method would not be viable for rubrene, as it will photo-oxidize during the evaporation of the solvent into a photo-inactive compound. The second method involved dissolving the chromophores in an organic solvent, adding an aqueous polymer solution, and heating it to evaporate the residual solvent from the water. Although initially tried with chloroform, which did not make homogeneously dissolved solutions, the method was interesting for green purposes as the organic solvent would be evaporated for the most part. Method 3 was similar to method 2, only now the solvent was not evaporated out of the water phase, this showed very much promise, as a clear dissolved solution was obtained, however, for green purposes, as little as possible organic solvent should be in the upconversion solution. Therefore, further experiments were done with method 2.

It was shown that method 2, with water-soluble solvents, resulted in the best-dissolved solutions. From the solvents tried, acetone showed to give the best results. DLS measurements showed that despite, the new sample preparation methods, aggregates were formed in the upconversion solution, which were caused by the chromophores in the solution. Therefore, still more optimization is needed to make a real homogeneously dissolved solution. Additionally, experiments should be done to see if the polymers migrate into the polymer, or if there is enough acetone left for the chromophores to be dissolved in the organic phase.

With the new sample preparation method, the influence of oxygen on the upconversion was investigated which did not show a large dependence, this was explained by the oxygen barrier that would be formed by the SCPNs.

Lastly, the influence of the use of different spectrometers was investigated, from which could be concluded that the fluorescence spectrometer used in this project is not suited for upconversion measure-

ments, especially the upconversion when excited at a wavelength above 570 nm.

As a demonstration, the most suited upconversion pair was chosen with which a photocatalytic trifluoromethylation of a phenylpyrrole substrate was performed. This reaction definitely needs optimization for the combination with upconversion as the reaction solution was completely opaque and the reaction showed to be very inefficient in product formation. However, the fact that the ^{19}F NMR spectra showed that product had been formed, and that nearly all initial product was disappeared leads to believe that, with optimization, catalysis using TTAUC is possible. This indicates the first step towards photocatalysis by upconversion in aqueous media.

Bibliography

[1] S. Baluschev, K. Katta, Y. Avlasevich, and K. Landfester, "Annihilation upconversion in nanoconfinement: solving the oxygen quenching problem," *Mater. Horiz*, vol. 3, pp. 478–486, 2016.

[2] B. D. Ravetz, A. B. Pun, E. M. Churchill, D. N. Congreve, T. Rovis, and L. M. Campos, "Photoredox catalysis using infrared light via triplet fusion upconversion," *Nature 2019 565:7739*, vol. 565, pp. 343–346, 1 2019.

[3] D. M. Arias-Rotondo and J. K. Mccusker, "Chem Soc Rev Chemical Society Reviews The photophysics of photoredox catalysis: a roadmap for catalyst design The photophysics of photoredox catalysis: a roadmap for catalyst design," *Chem. Soc. Rev*, vol. 45, p. 5803, 2016.

[4] T. Welton, "Solvents and sustainable chemistry," *Proceedings of the Royal Society A: Mathematical, Physical and Engineering Sciences*, vol. 471, 11 2015.

[5] N. J. Turro, *Modern Molecular Photochemistry*. Mill Valley: University Science Books, 1991.

[6] F. Eisenreich, T. H. Kuster, D. van Krimpen, and A. R. Palmans, "Photoredox-Catalyzed Reduction of Halogenated Arenes in Water by Amphiphilic Polymeric Nanoparticles," *Molecules (Basel, Switzerland)*, vol. 26, 10 2021.

[7] W. Van Vliet, "Photon up-conversion in water by encapsulation of sensitizer and emitter units in single-chain polymeric nanoparticles.," 2021.

[8] "Visible Light Photoredox Catalysts — TCI AMERICA." Available at: https://www.tcichemicals.com/US/en/c/12998.

[9] D. J. Griffiths and D. F. Schroeter, *Introduction to Quantum Mechanics*. Cambridge University Press, 8 2018.

[10] "Ch21b_Lecture14_2018." Available at: http://web.gps.caltech.edu/~gab/ch21b/docs/Ch21b_Lecture14_2018.pdf.

[11] "Why are singlet to triplet transitions forbidden? - Quora." Available at: https://www.quora.com/Why-are-singlet-to-triplet-transitions-forbidden.

[12] P. Atkins and J. Paulo, *Physical Chemistry*. Oxford University press, 11th edition ed., 2008.

[13] C. M. Marian, "Understanding and Controlling Intersystem Crossing in Molecules," *Annual Review of Physical Chemistry*, 2021.

[14] G. A. Jones and D. S. Bradshaw, "Resonance Energy Transfer: From Fundamental Theory to Recent Applications," *Frontiers in Physics*, vol. 7, 2019.

[15] "Dexter Energy Transfer - Chemistry LibreTexts." Available at: https://chem.libretexts.org/Bookshelves/Physical_and_Theoretical_Chemistry_Textbook_Maps/Supplemental_Modules_(Physical_and_Theoretical_Chemistry)/Fundamentals/Dexter_Energy_Transfer.

[16] Y. C. Simon and C. Weder, "Low-power photon upconversion through triplet–triplet annihilation in polymers," *Journal of Materials Chemistry*, vol. 22, pp. 20817–20830, 9 2012.

[17] D. G. Bossanyi, Y. Sasaki, S. Wang, D. Chekulaev, N. Kimizuka, N. Yanai, and J. Clark, "Spin Statistics for Triplet–Triplet Annihilation Upconversion: Exchange Coupling, Intermolecular Orientation, and Reverse Intersystem Crossing," *JACS Au*, vol. 1, pp. 2188–2201, 12 2021.

[18] Y. Y. Cheng, B. Fückel, T. Khoury, R. G. Clady, M. J. Tayebjee, N. J. Ekins-Daukes, M. J. Crossley, and T. W. Schmidt, "Kinetic analysis of photochemical upconversion by triplet-triplet annihilation: Beyond any spin statistical limit," *Journal of Physical Chemistry Letters*, vol. 1, pp. 1795–1799, 6 2010.

[19] Y. Zhou, F. N. Castellano, T. W. Schmidt, and K. Hanson, "On the Quantum Yield of Photon Upconversion via Triplet-Triplet Annihilation," *ACS Energy Letters*, vol. 5, pp. 2322–2326, 7 2020.

[20] N. A. Durandin, J. Isokuortti, A. Efimov, E. Vuorimaa-Laukkanen, N. V. Tkachenko, and T. Laaksonen, "Critical Sensitizer Quality Attributes for Efficient Triplet-Triplet Annihilation Upconversion with Low Power Density Thresholds," *Journal of Physical Chemistry C*, vol. 123, pp. 22865–22872, 9 2019.

[21] D. Meroni, A. Monguzzi, and F. Meinardi, "Photon upconversion in multicomponent systems: Role of back energy transfer," *The Journal of Chemical Physics*, vol. 153, p. 114302, 9 2020.

[22] J. Isokuortti, S. R. Allu, A. Efimov, E. Vuorimaa-Laukkanen, N. V. Tkachenko, S. A. Vinogradov, T. Laaksonen, and N. A. Durandin, "Endothermic and Exothermic Energy Transfer Made Equally Efficient for Triplet-Triplet Annihilation Upconversion," *Journal of Physical Chemistry Letters*, vol. 11, pp. 318–324, 1 2020.

[23] Y. Y. Cheng, B. Fückel, T. Khoury, R. G. Clady, N. J. Ekins-Daukes, M. J. Crossley, and T. W. Schmidt, "Entropically driven photochemical upconversion," *Journal of Physical Chemistry A*, vol. 115, pp. 1047–1053, 2 2011.

[24] L. Huang, T. Le, K. Huang, and G. Han, "Enzymatic enhancing of triplet–triplet annihilation upconversion by breaking oxygen quenching for background-free biological sensing," *Nature Communications 2021 12:1*, vol. 12, pp. 1–9, 3 2021.

[25] B. Zhou, B. Tang, C. Zhang, C. Qin, Z. Gu, Y. Ma, T. Zhai, and J. Yao, "Enhancing multiphoton upconversion through interfacial energy transfer in multilayered nanoparticles," *Nature Communications 2020 11:1*, vol. 11, pp. 1–9, 3 2020.

[26] S. Penczek and J. B. Pretula, "Fundamental Aspects of Chain Polymerization," *Polymer Science: A Comprehensive Reference, 10 Volume Set*, vol. 3, pp. 3–38, 1 2012.

[27] R. B. Grubbs and R. H. Grubbs, "50th Anniversary Perspective: Living Polymerization - Emphasizing the Molecule in Macromolecules," *Macromolecules*, vol. 50, pp. 6979–6997, 9 2017.

[28] C. Schaller, "6.10 Living Radical Polymerisation," 5 2021. Available at: https://chem.libretexts.org/@go/page/202842.

[29] J. Yeow, R. Chapman, A. J. Gormley, and C. Boyer, "Up in the air: oxygen tolerance in controlled/living radical polymerisation," *Chemical Society Reviews*, vol. 47, pp. 4357–4387, 6 2018.

[30] M. Chen, G. Moad, and E. Rizzardo, "Thiocarbonylthio end group removal from RAFT-synthesized polymers by a radical-induced process," *Journal of Polymer Science Part A: Polymer Chemistry*, vol. 47, pp. 6704–6714, 12 2009.

[31] P. Y. Bruice, *Organic chemistry*. Pearson, 8th edition ed., 2016.

[32] L. Q. Xu, H. Jiang, K. G. Neoh, E. T. Kang, and G. D. Fu, "Poly(dopamine acrylamide)-co-poly(propargyl acrylamide)-modified titanium surfaces for 'click' functionalization," *Polymer Chemistry*, vol. 3, pp. 920–927, 3 2012.

[33] F. Eisenreich and A. R. A. Palmans, "Direct C-H trifluoromethylation of (hetero)arenes in water enabled by photoredox-active amphiphilic nanoparticles." 2022.

[34] E. Huerta, P. J. Stals, E. W. Meijer, and A. R. Palmans, "Consequences of Folding a Water-Soluble Polymer Around an Organocatalyst," *Angewandte Chemie International Edition*, vol. 52, pp. 2906–2910, 3 2013.

[35] Y. Liu, S. Pujals, P. J. Stals, T. Paulöhrl, S. I. Presolski, E. W. Meijer, L. Albertazzi, and A. R. Palmans, "Catalytically Active Single-Chain Polymeric Nanoparticles: Exploring Their Functions in Complex Biological Media," *Journal of the American Chemical Society*, vol. 140, pp. 3423–3433, 3 2018.

[36] J. T. Ly, S. A. Lopez, J. B. Lin, J. J. Kim, H. Lee, E. K. Burnett, L. Zhang, A. Aspuru-Guzik, K. N. Houk, and A. L. Briseno, "Oxidation of rubrene, and implications for device stability," *Journal of Materials Chemistry C*, vol. 6, pp. 3757–3761, 4 2018.

[37] S. N. Sanders, M. K. Gangishetty, M. Y. Sfeir, and D. N. Congreve, "Photon Upconversion in Aqueous Nanodroplets," *J. Am. Chem. Soc.*, vol. 141, no. 23, pp. 9180–9184, 2019.

[38] "Togni-s-Reagent-CAS-887144-97-0-FNMR.jpg (660×466)." Available at: https://www.watson-int.com/wp-content/uploads/2013/03/Togni-s-Reagent-CAS-887144-97-0-FNMR.jpg.

A. Appendix

A.1. Polymer synthesis
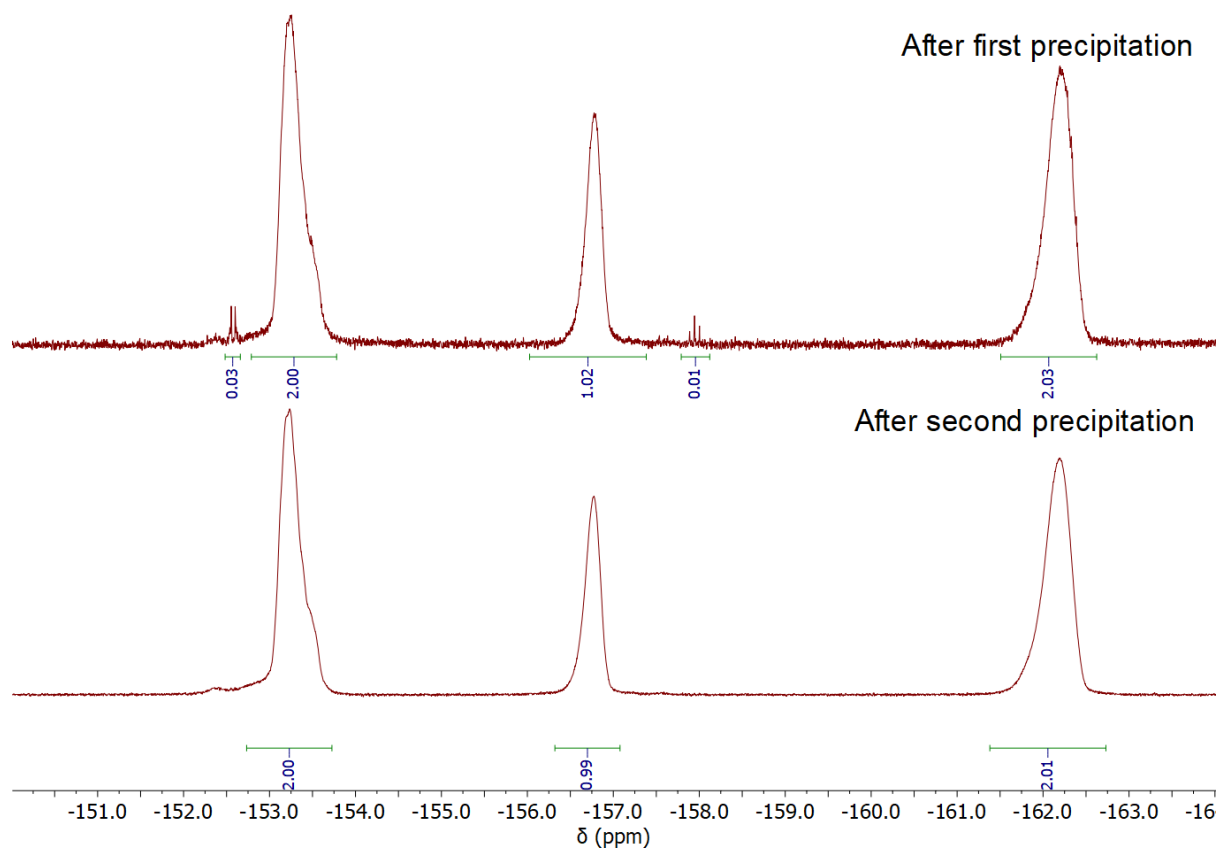
Figure A.1.: ^{19}F NMR (376 MHz, CDCl$_3$) of **C** after first and second precipitation

Table A.1.: Dodecyl content calculated from Figure3.16 with the different pairs of peaks. For **P1** the averages were taken over pairs a and d and b and e.

Polymer	a and d (%)	b and e (%)	c and f (%)	average (%)
P1	22.0	21.6	19.1	22
P2	32.9	32.7	33.1	33
P3	44.1	43.8	43.2	44
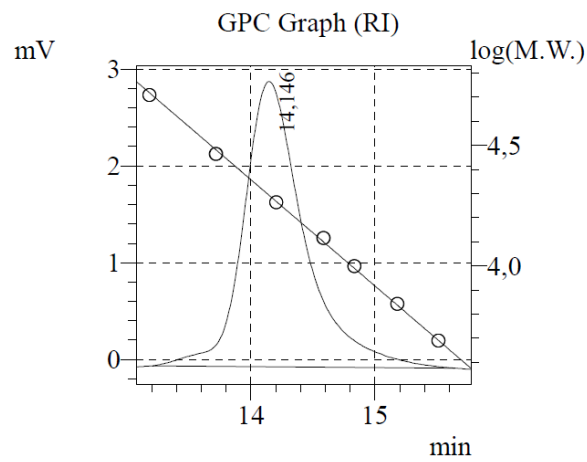
Figure A.2.: SEC chromatogram of **C** in THF ($c = 1$ mg mL^{-1})

Table A.2.: Hydrodynamic diameters of the largest intensity peaks from the DLS measurements given in Figure 3.17

Polymer	Peak 1		Peak 2	
	$D_H\pm$standard deviation (nm)	Intensity (%)	$D_H\pm$standard deviation (nm)	Intensity (%)
P1	11 ± 2	100		
P2	13 ± 3	100		
P3	14 ± 4	84	$(1.5 \pm 0.8) \cdot 10^2$	16
P4	13 ± 3	96	$(4 \pm 2) \cdot 10^3$	4
P5	11 ± 3	90	$(1.8 \pm 0.9) \cdot 10^2$	9
P6	16 ± 7	90	$(3 \pm 1) \cdot 10^2$	8
P7	11 ± 2	29	$(1.6 \pm 0.5) \cdot 10^2$	60
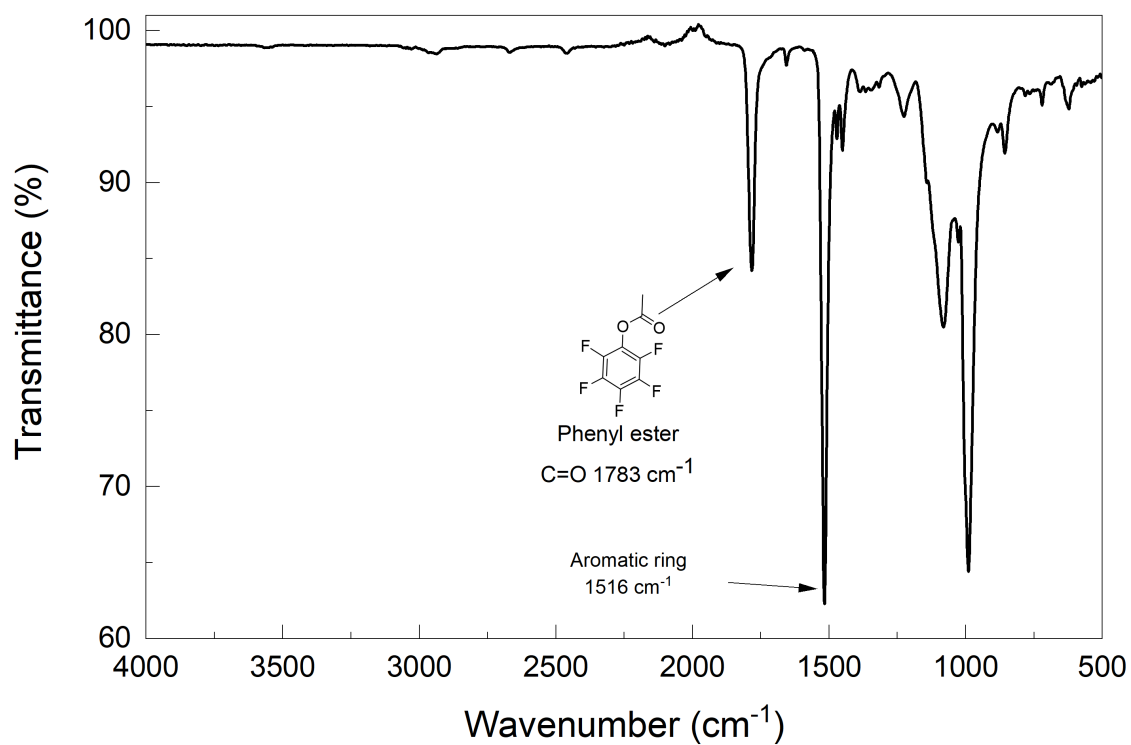
Figure A.3.: FTIR of **C**.
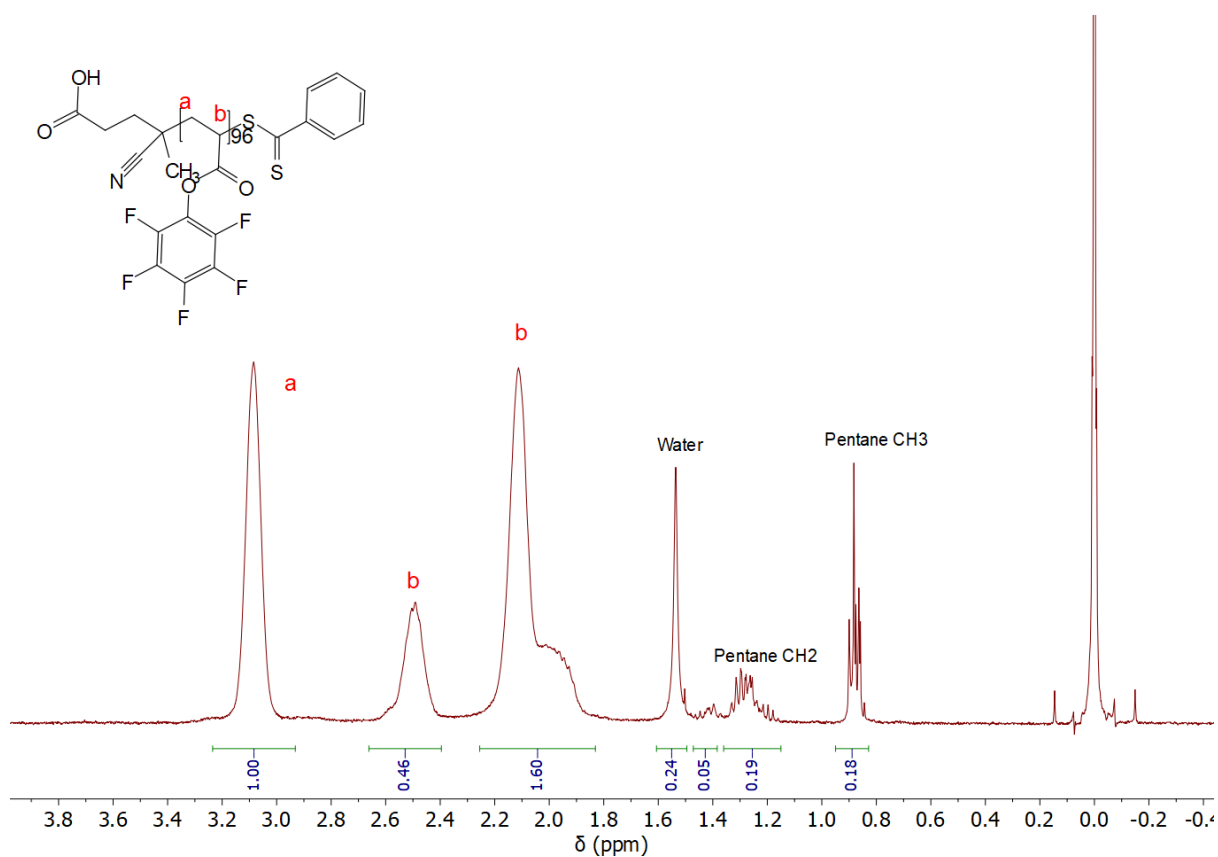
Figure A.4.: ^{1}H NMR (400 MHz CDCl$_3$) of **C**.
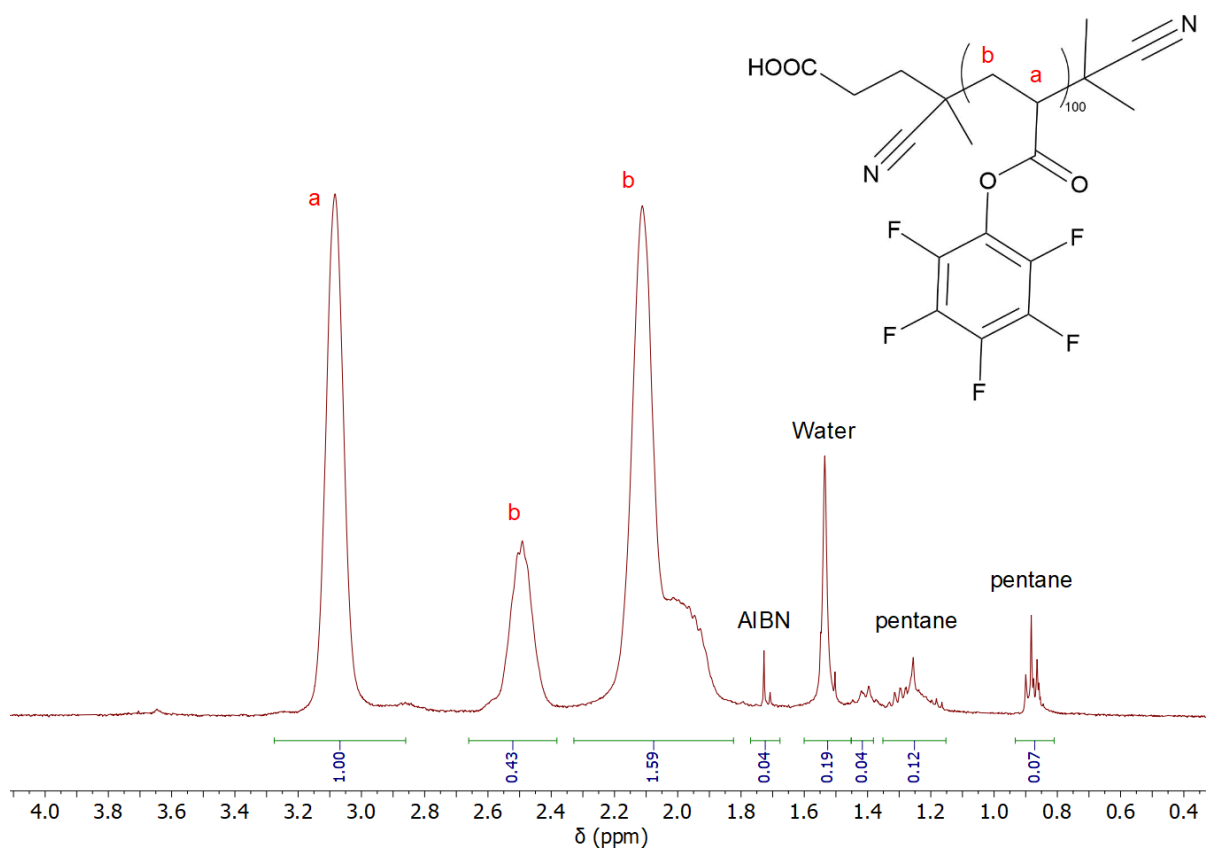
Figure A.5.: ^{1}H NMR (400 MHz CDCl$_3$) of **D**
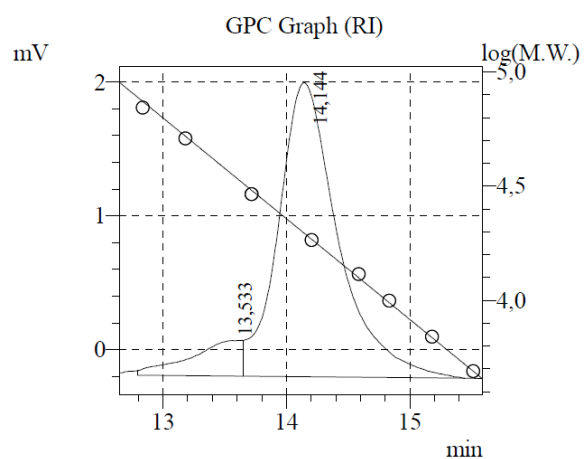
Figure A.6.: SEC in THF on **D**. ($c = 1$ mg/mL, injection volume 30 µL.)
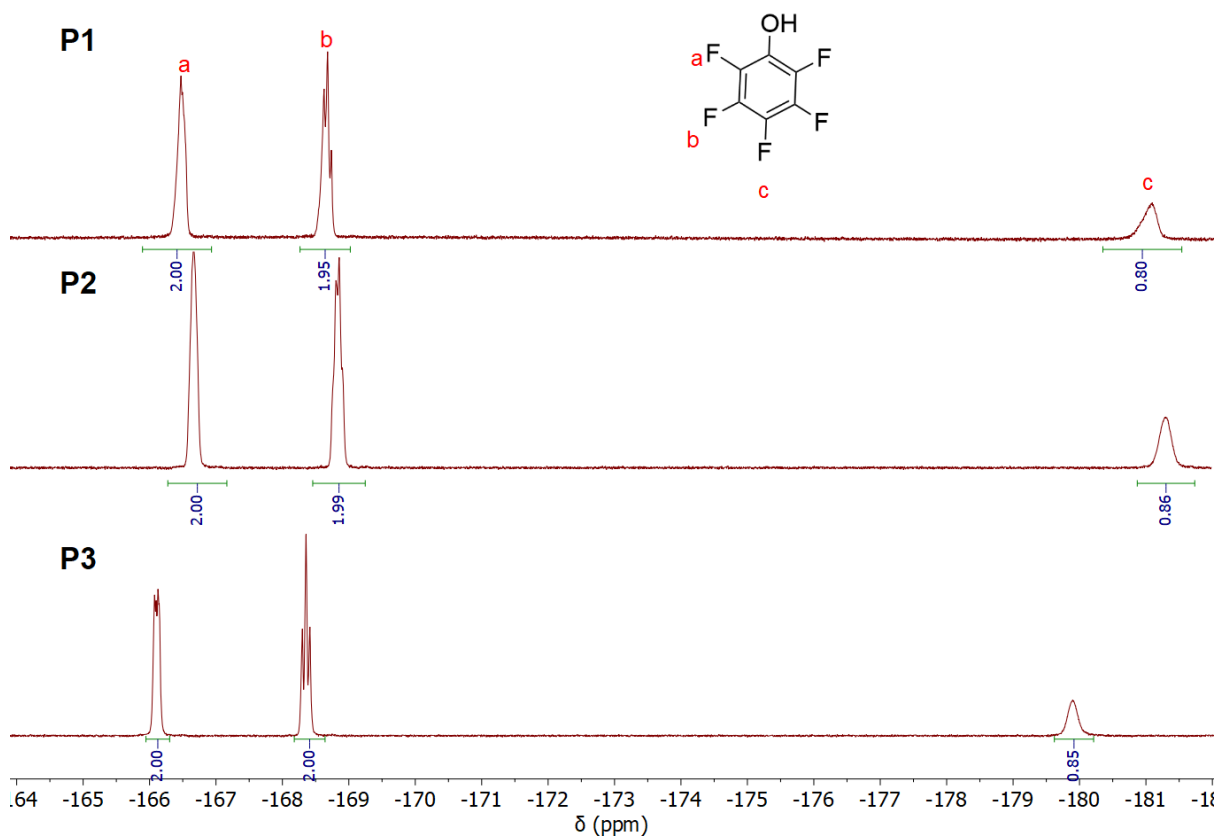
Figure A.7.: ^{19}F NMR (376 MHz, CDCl$_3$) of the reaction solution after 5 h of reaction with Jeffamine.
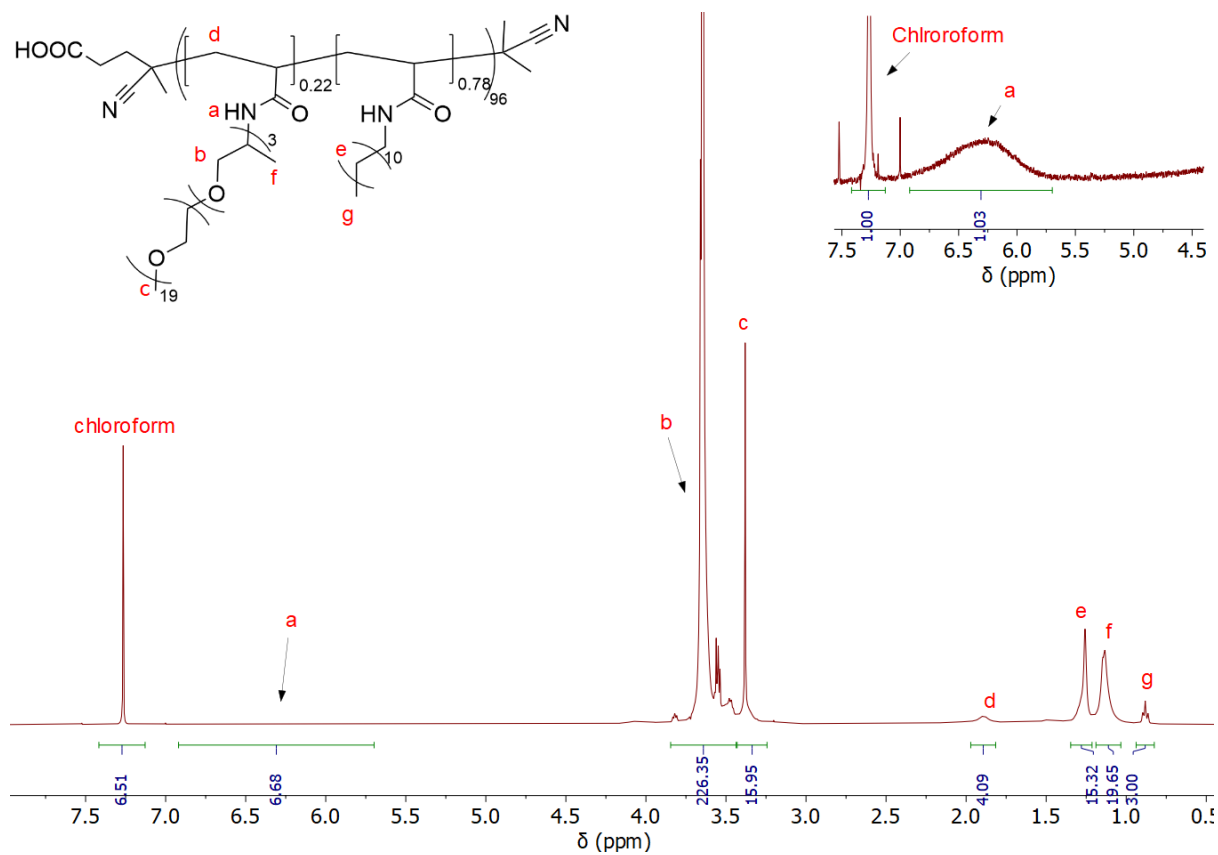
Figure A.8.: ^{1}H NMR (400 MHz CDCl$_3$) of **P1**
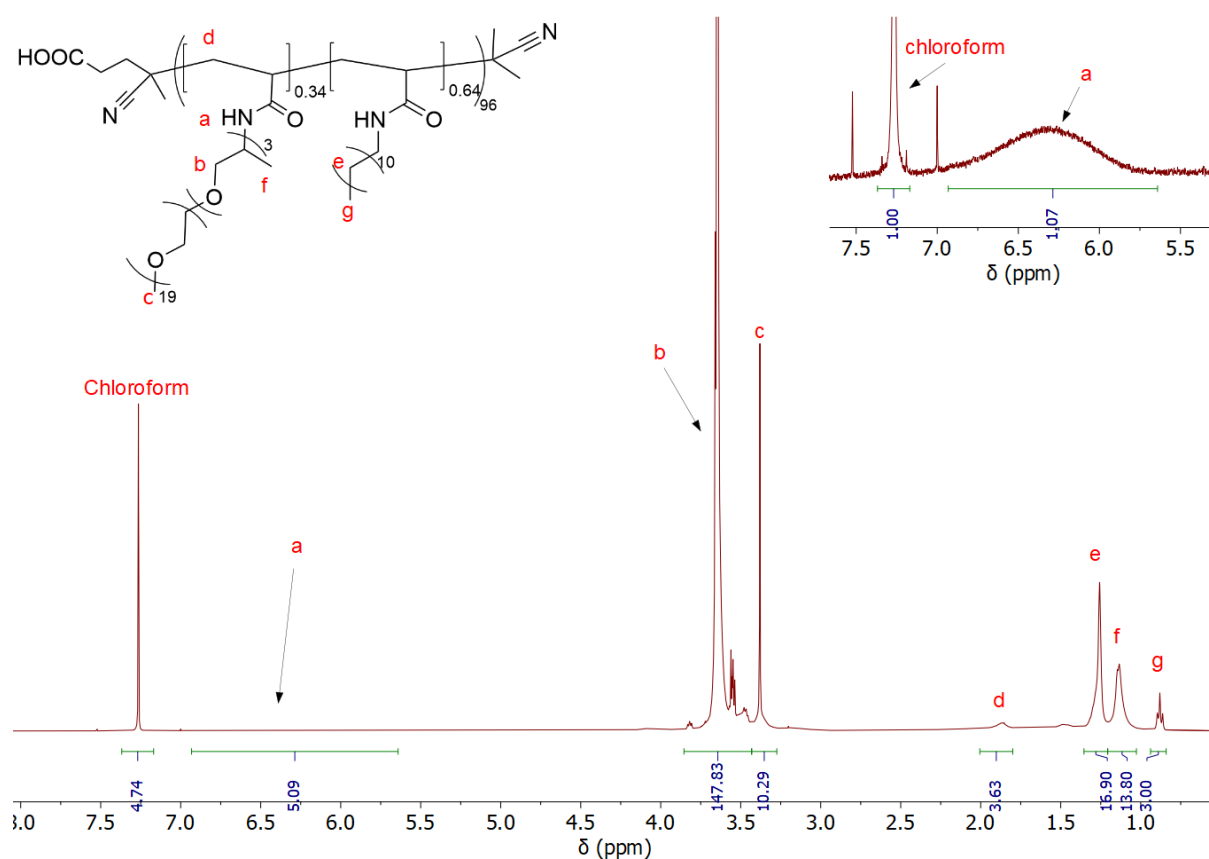
Figure A.9.: ^{1}H NMR (400 MHz CDCl$_3$) of **P2**
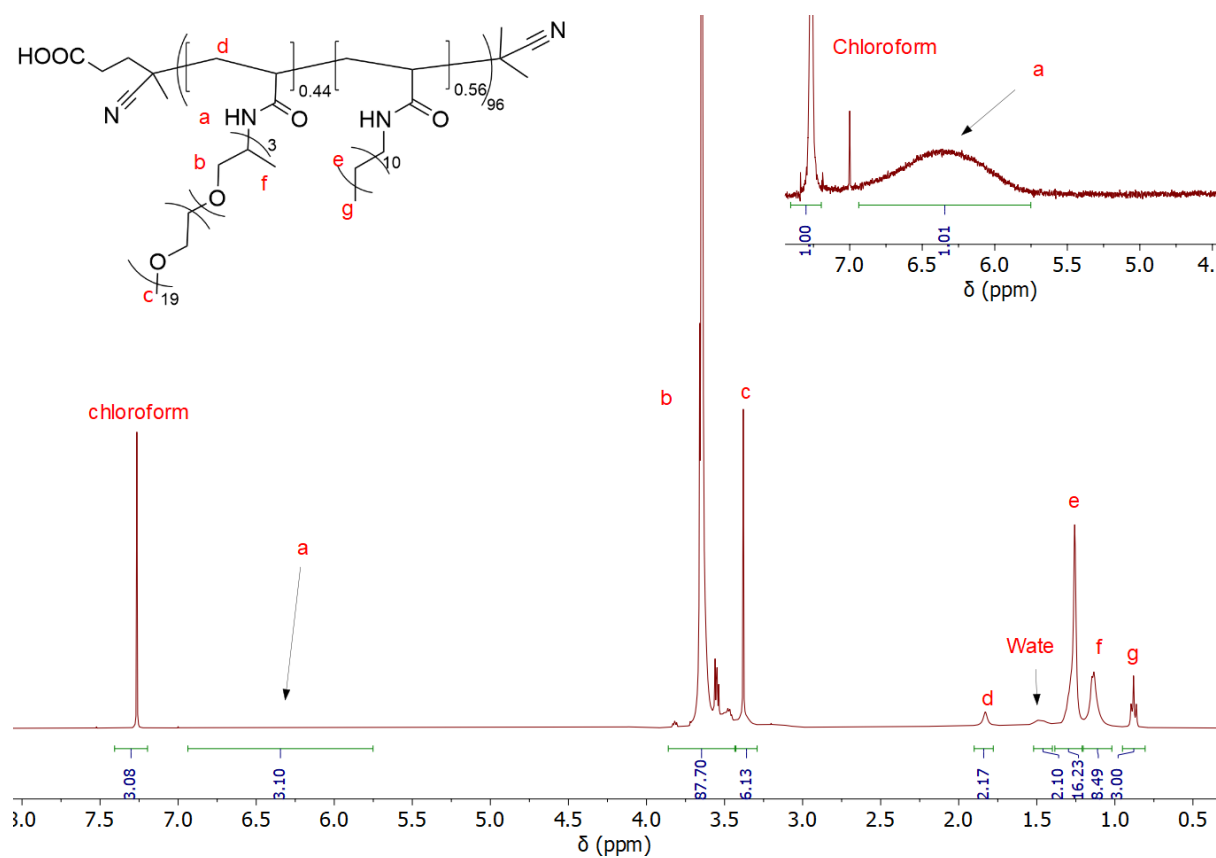
Figure A.10.: ^{1}H NMR (400 MHz CDCl$_3$) of **P3**
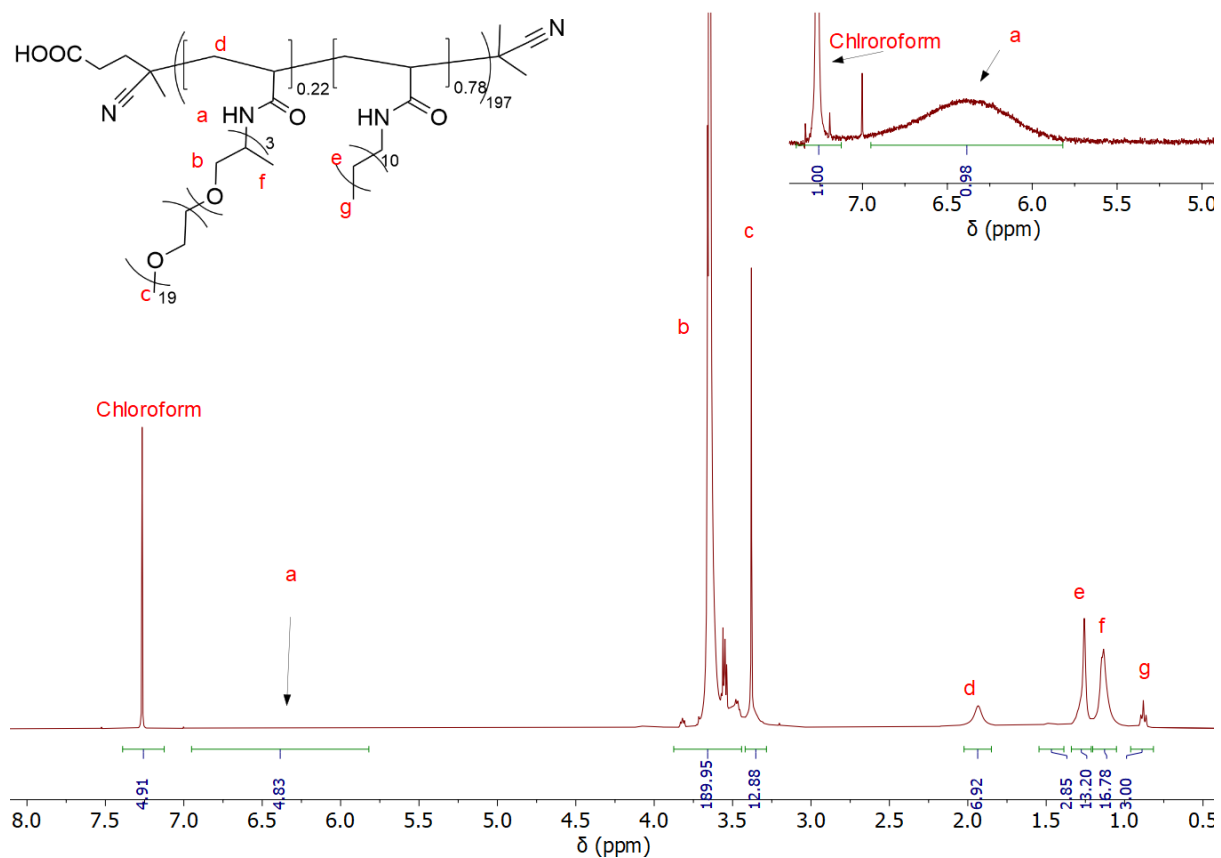
Figure A.11.: ^{1}H NMR (400 MHz CDCl$_3$) of **P4**
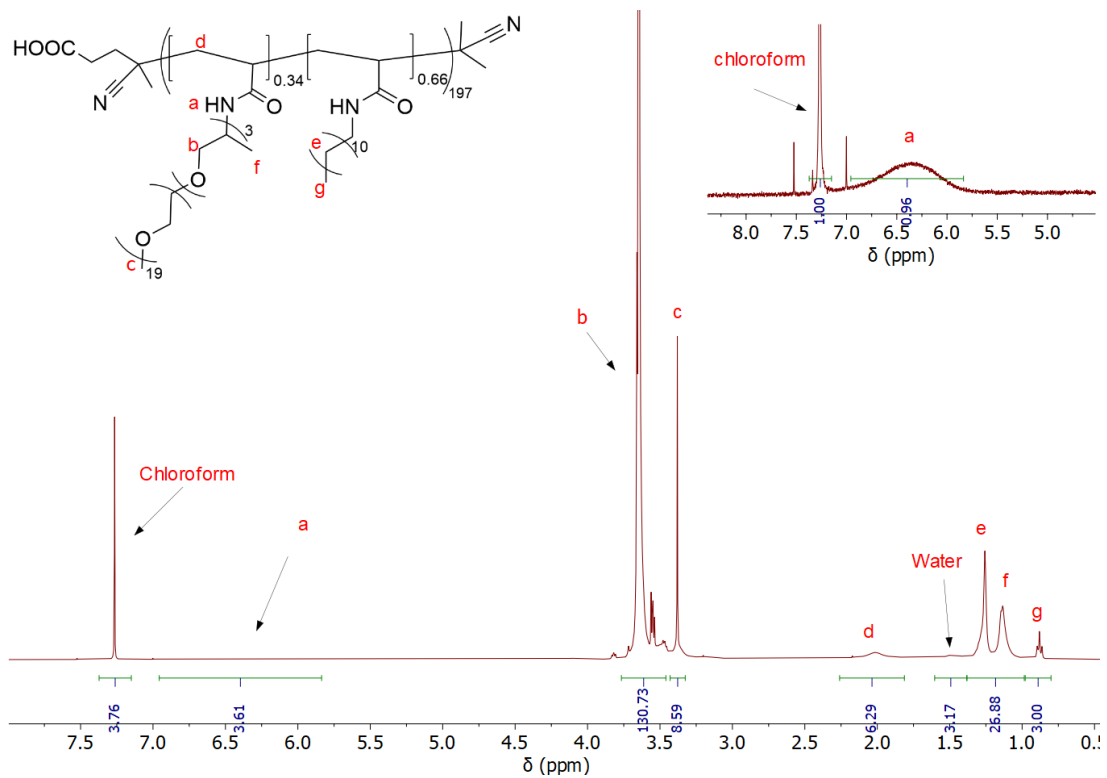
Figure A.12.: ^{1}H NMR (400 MHz CDCl$_3$) of **P5**
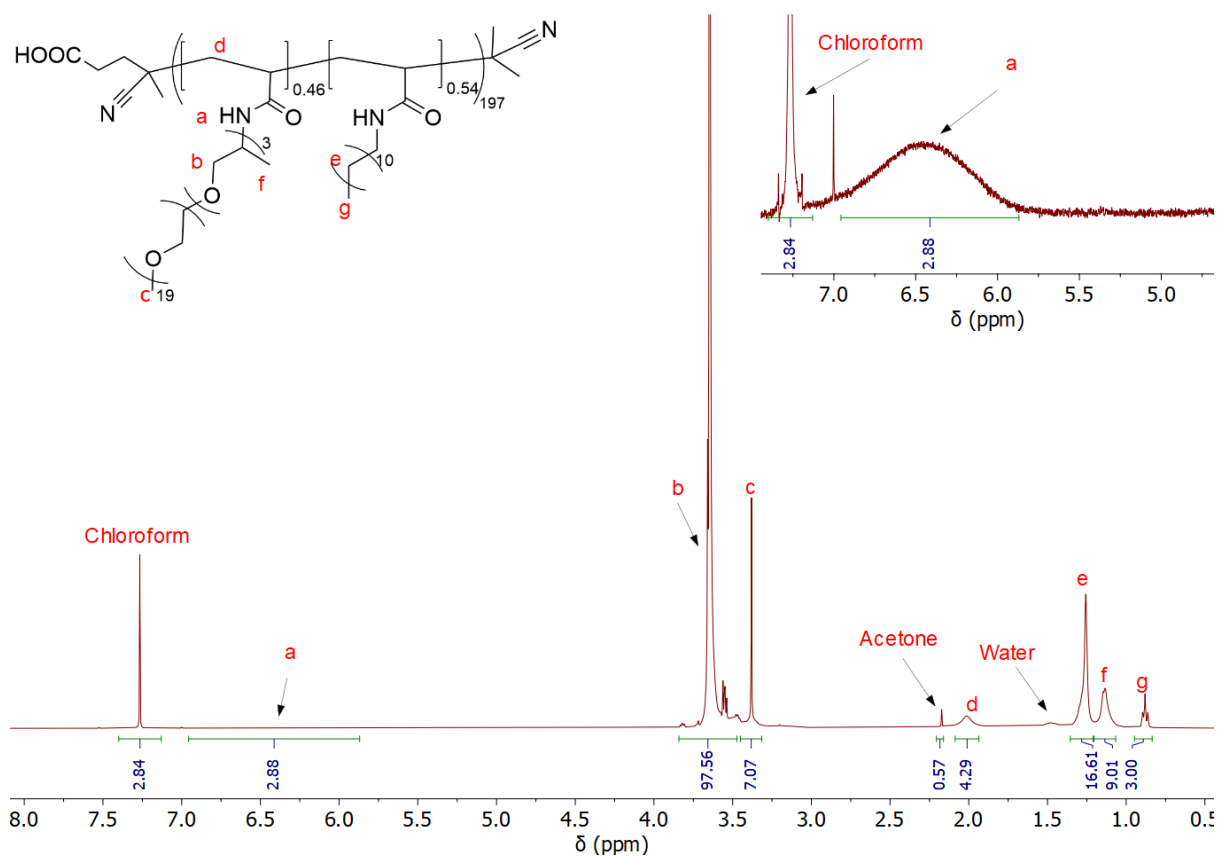
Figure A.13.: ^{1}H NMR (400 MHz CDCl$_3$) of **P6**
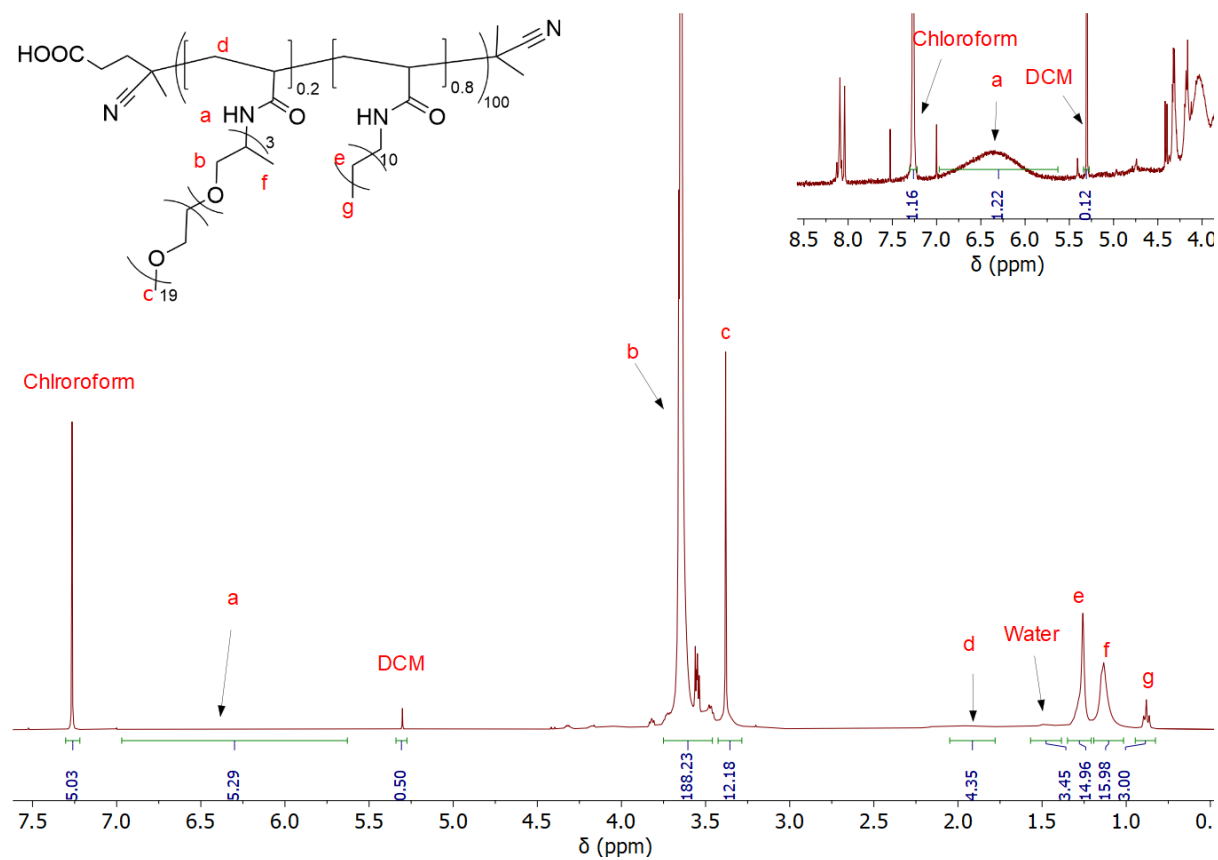
Figure A.14.: ^{1}H NMR (400 MHz CDCl$_3$) of **P7**
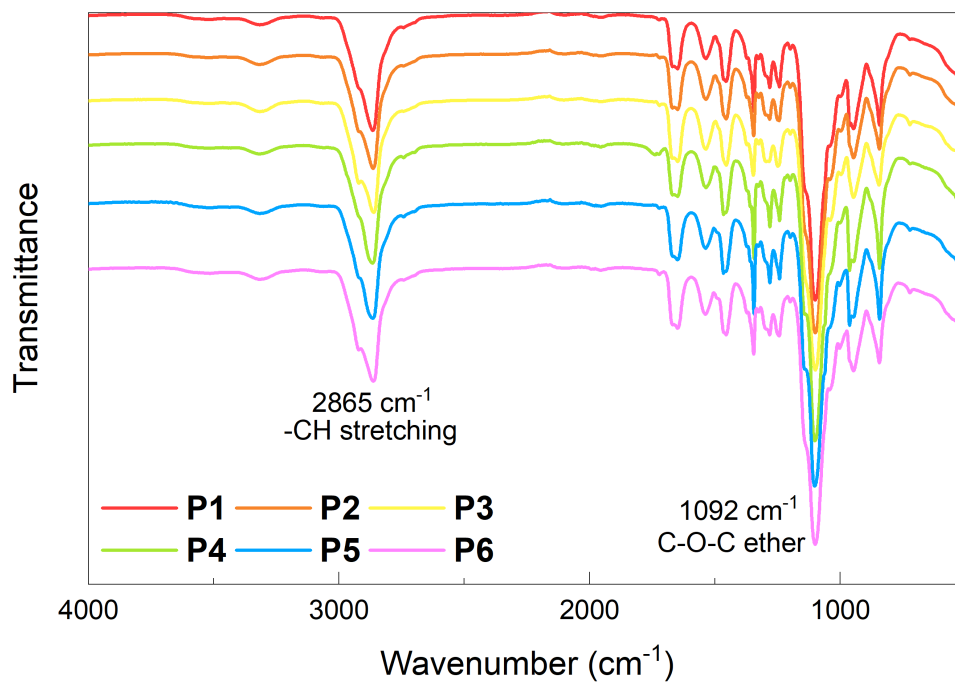
Figure A.15.: FT-IR spectra of **P1**-**P7**.
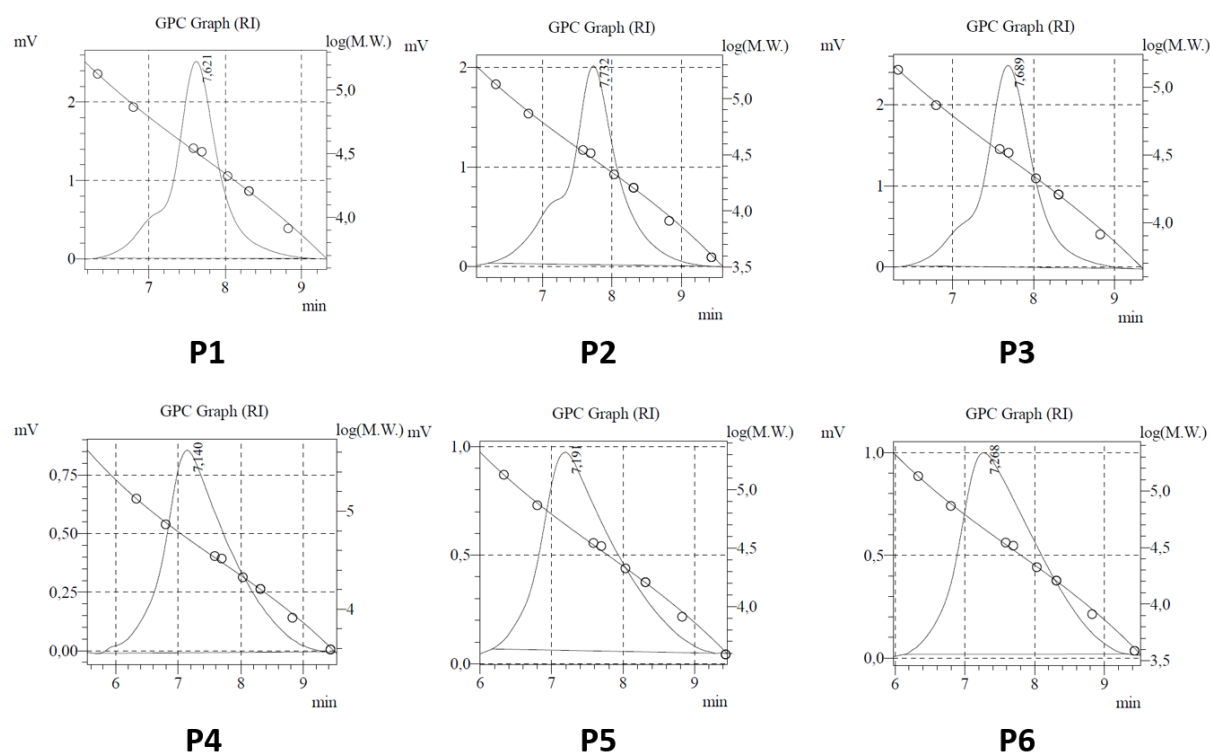
Figure A.16.: Results of SEC measurements on **P1**-**P7** in DMF. ($c = 1$ mg/mL, injection volume 30 µL.)
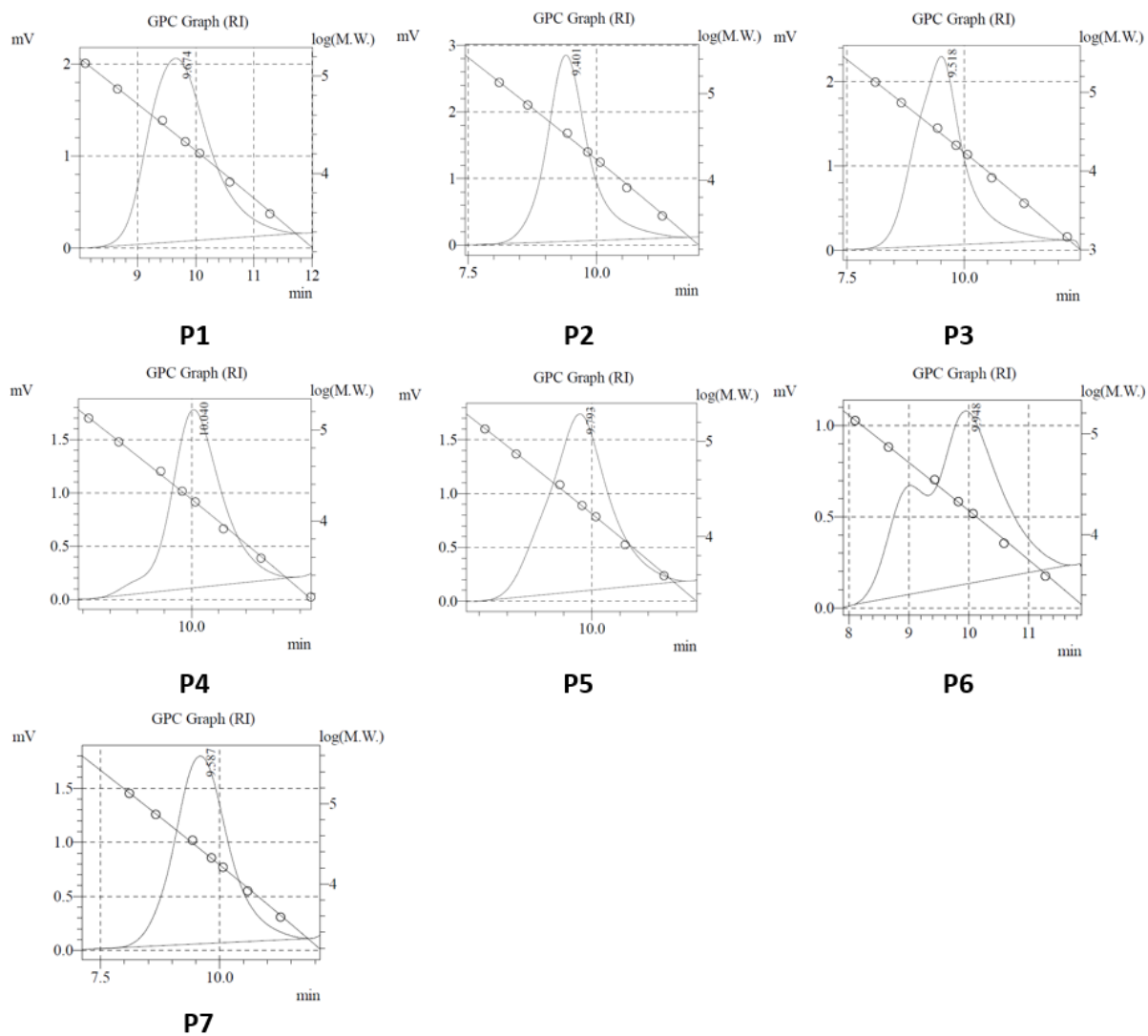
Figure A.17.: Results of SEC measurements on **P1-P7** in PBS. ($c = 1$ mg/mL, injection volume 20 µL.)
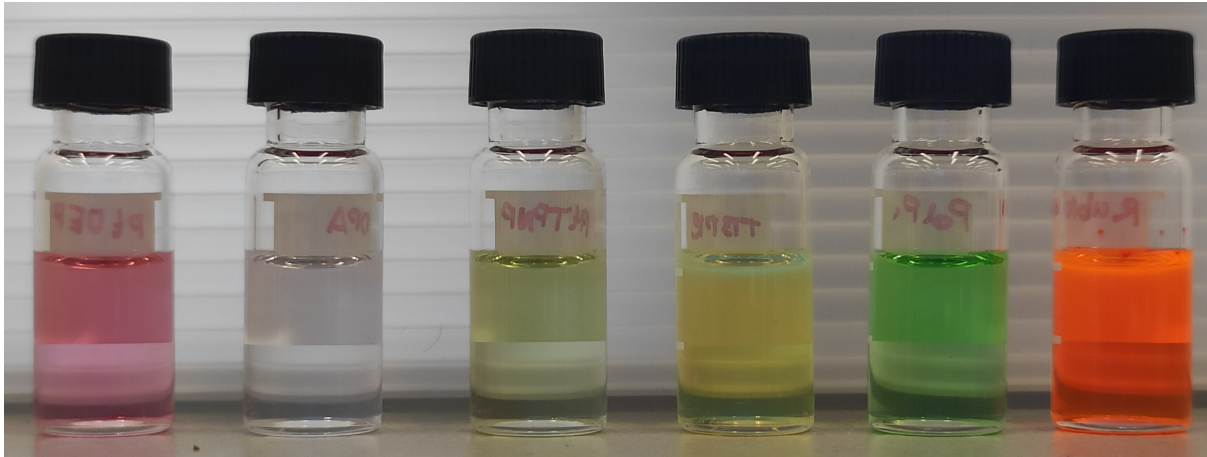
A.2. Chromophores

Figure A.18.: Image of the used chromophores, dissolved in chloroform. FLTR: **S1**, **E1** , **S2**, **E2**, **S3**, **E3** ($c = 0.022$ mg/mL, 0.275 mg/mL, 0.039 mg/mL, 0.373 mg/mL, 0.035 mg/mL, 0.639 mg/mL resepctively.)

A.3. Upconversion
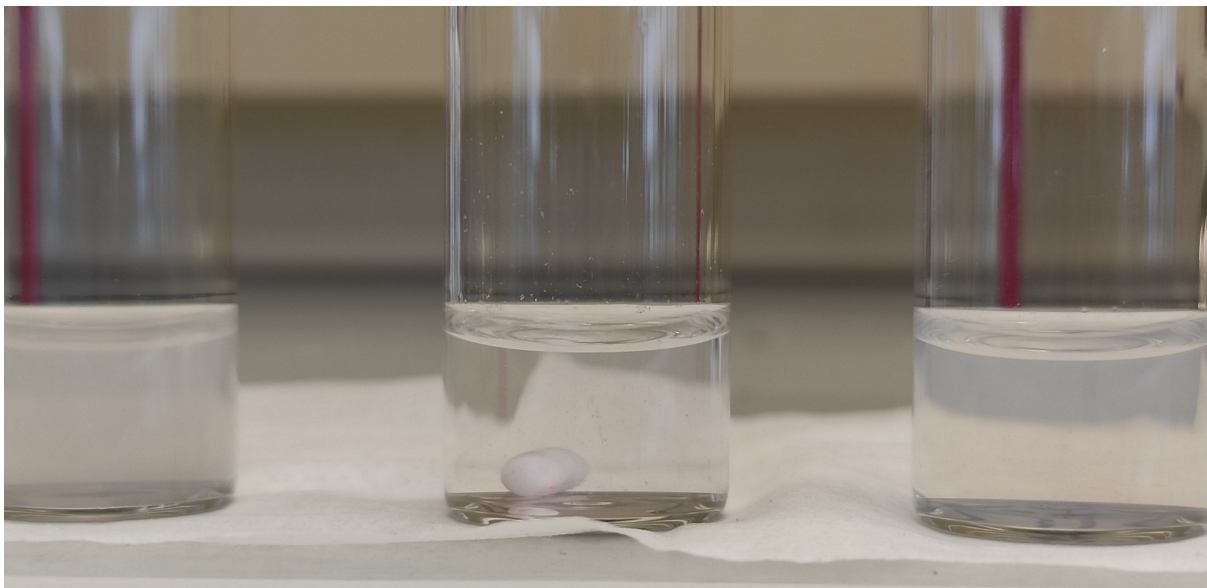
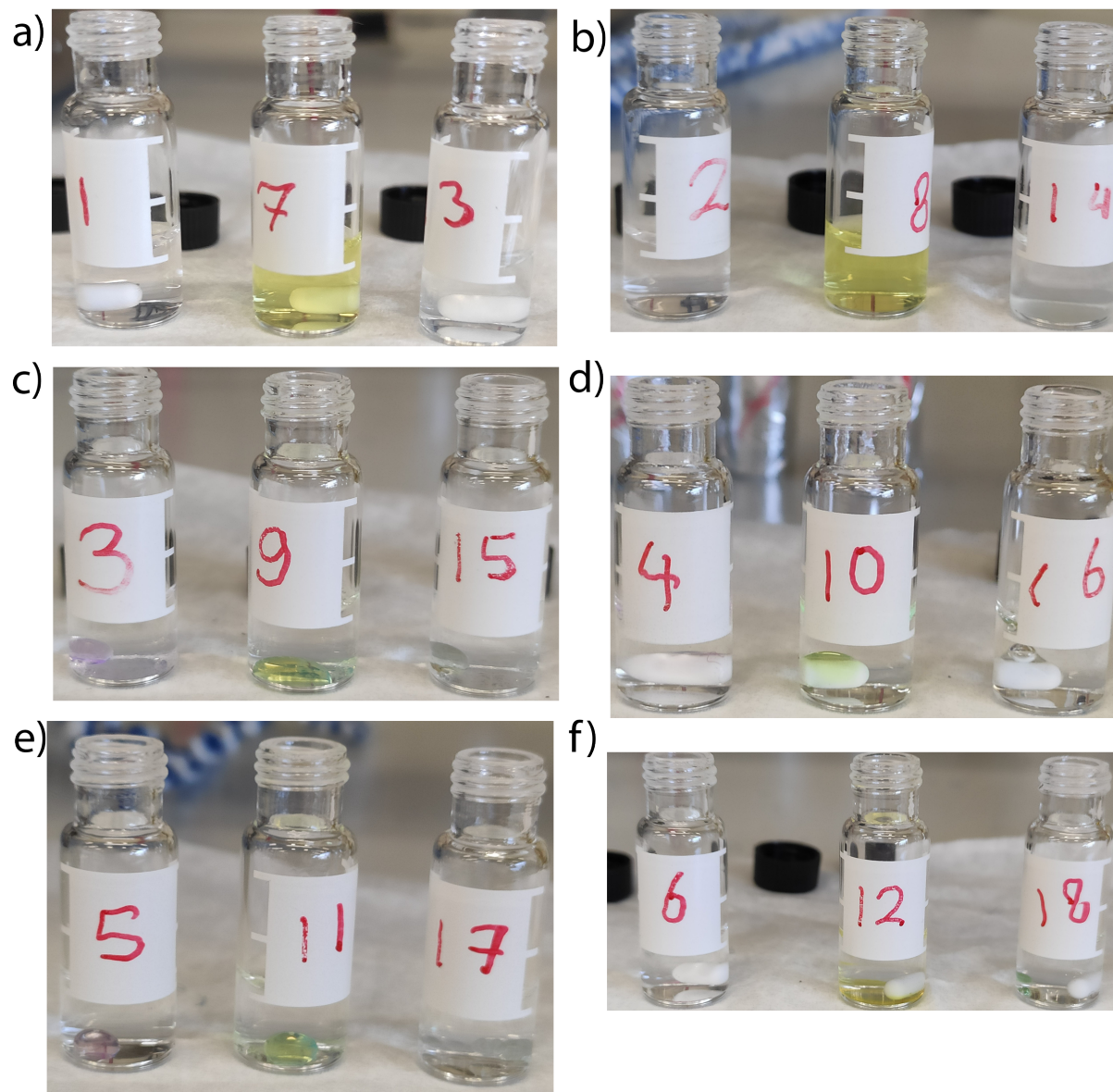**Figure A.19.:** Picture of the resulting solutions made by using FLTR: method 1, method 2, and method 3.

Figure A.20.: Pictures of the solutions of Figure 5.3 before heating. Samples are prepared with a) THF, b) acetone, c) chloroform, d) benzene, e) DCM, and f) without any organic solvent. Left: upconversion pair 1, middle: upconversion pair 2, upconversion pair 3.
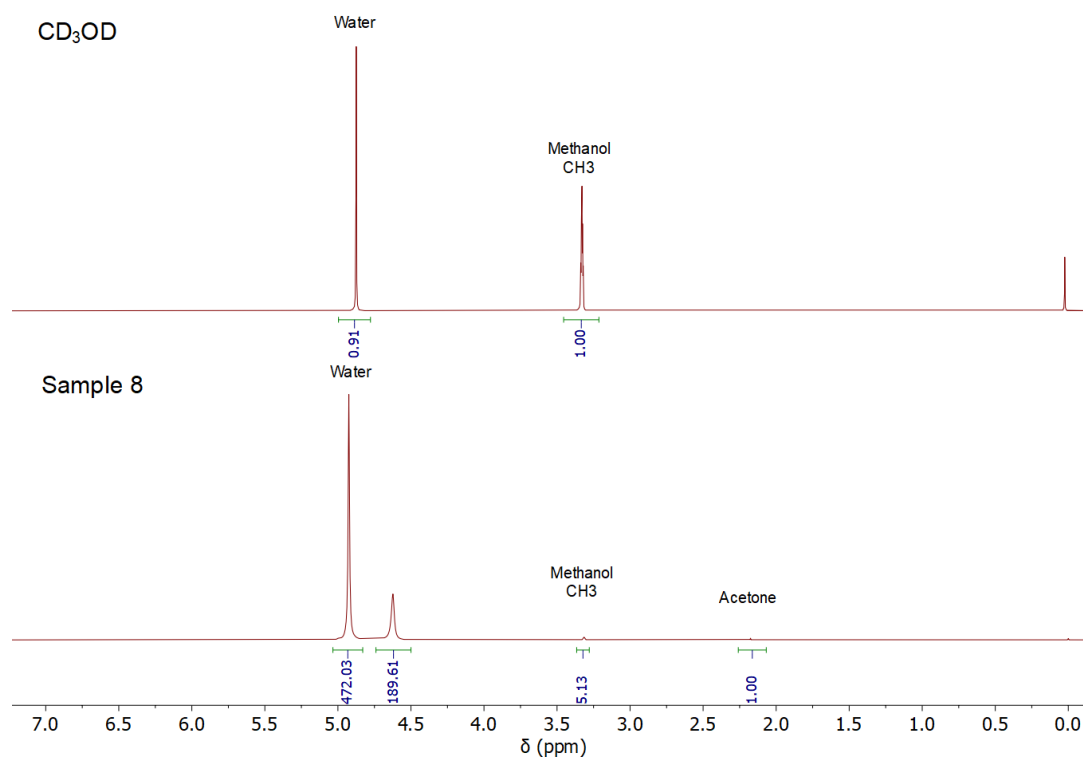
Figure A.21.: ^{1}H NMR (400 MHz, CD$_3$OD) spectra of CD$_3$OD and sample 8 to check the concentration acetone in sample 8. From the spectrum of the CD$_3$OD, it is determined that the ratio between the water peak and the methanol peak is 0.907. Which means that in any measurement a water peak is present that is at least 91% of the methanol integral, if the integral is greater, the water is comming from the measured sample. Therefore, from the spectrum of sample 8, the part of the water peak comming from the solvent is $0.9071 \cdot 5.1303 = 4.65$ ppm and thus $472.03 - 4.65 = 467.38$ ppm of the water peak comes from the sample itself. Accounting for the amount of protons per acetone and water molecule, the concentration of acetone in water is calculated to be $1 \cdot 1/6/(1 \cdot 1/6 + 467.38 \cdot 1/2) \cdot 100\% = 0.071$mol%. The initial concentration of acetone was 10 vol% = 2.4 mol%, hence 97% of the acetone is evaporated.
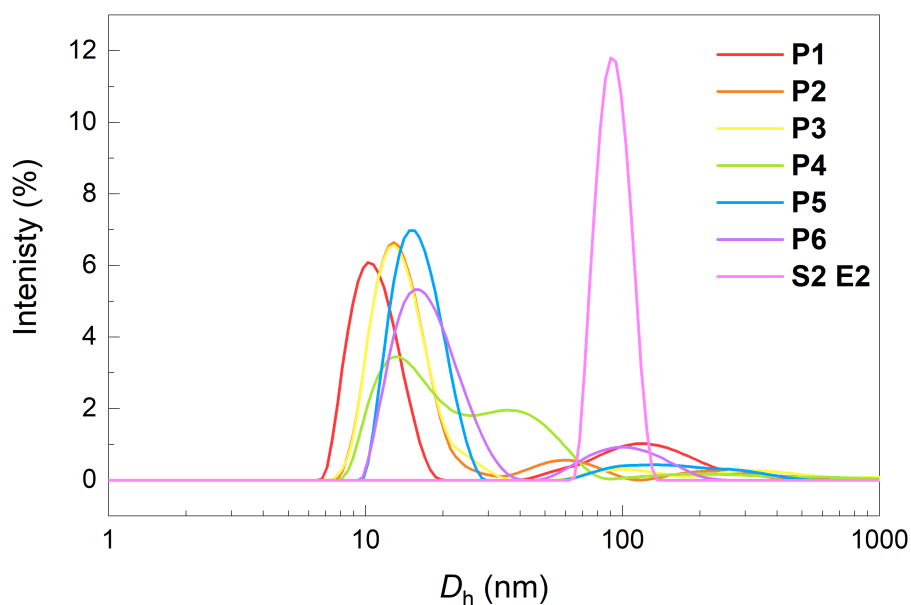

Figure A.22.: Size distribution of an aqueous polymer solution ($c = 1$ mg/mL) to which acetone was added (**P1-P6**), and **S2 E2** dissolved in acetone added to water.

Figure A.23.: Photograph of the solutions used to obtain the PL spectra of Figure 5.5. Left: **P4S1E1**, middle: **P5S2E2**, and right: **P5S3E3**.

Figure A.24.: Photograph of the solutions made for DLS measurements of Figure 5.4. FLTR: **P1-P6**.

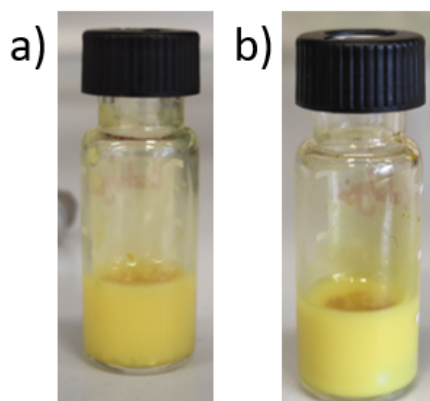## A.4. Photo-redox catalysis

Figure A.25.: Photographs of the solution used for the photocatalytic reaction with a) before reaction and b) after reaction.
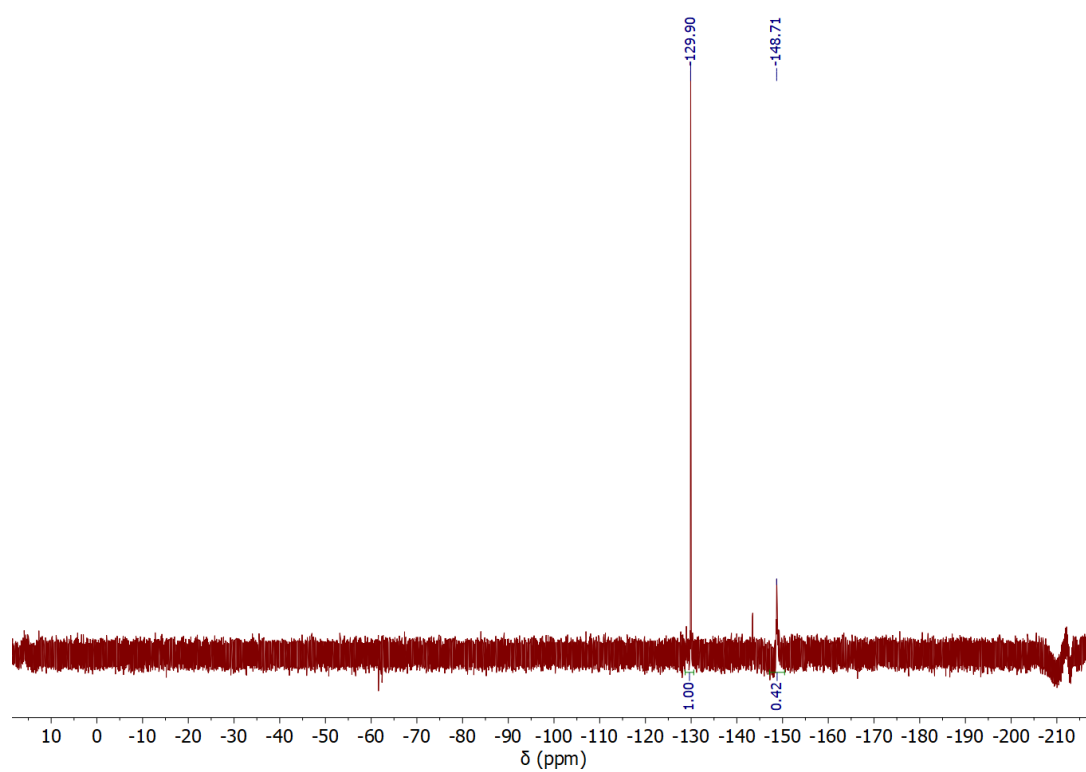

Figure A.26.: ^{19}F NMR (367 MHz D$_2$O) of the aqeuous layer of the extraction.